SLAC-52
UC-28, Particle Accelerators
and High-Voltage Machines
UC-34, Physics
TID-4500 (46th Ed.)

A SUBNANOSECOND COINCIDENCE CIRCUIT

November 1965

by

Arpad Barna

Technical Report
Prepared Under
Contract AT(04-3)-515
for the USAEC
San Francisco Operations Office

Printed in USA. Price $3.00. Available from Clearinghouse for Federal Scientific and Technical Information (CFSTI), National Bureau of Standards, U. S. Department of Commerce, Springfield, Virginia.

PREFACE

The electron beam at the two-mile accelerator of Stanford University is accelerated by a radio-frequency power at 2856 MHz. As a result, the beam consists of bunches separated by approximately 0.3 nsec. In order to be able to distinguish between particles originating from adjacent bunches, a coincidence circuit with a resolving time of 0.3 nsec is desired. Also, because of the unusually high instantaneous rates, it is necessary that the dead time of such a circuit be short. The development of a coincidence circuit with a resolving time of 0.3 nsec and a dead time of 10 nsec is the subject of this report.

The work was performed under the supervision of Prof. Robert R. Buss, whose helpful guidance has been deeply appreciated. The help provided by Prof. Martin L. Perl who also established the specifications is gratefully acknowledged. The progress of this project was furthered by stimulating discussions with Prof. Burton Richter. Invaluable assistance in the construction and in the measurements came from Mr. C. Richard Carman.

The work was supported by the U. S. Atomic Energy Commission.

TABLE OF CONTENTS

LIST OF FIGURES

LIST OF FIGURES - (continued)

LIST OF FIGURES - (continued)

Page

LIST OF TABLES

I. INTRODUCTION: PRIOR TECHNOLOGY

Coincidence circuits in physics experiments serve the purpose of detecting when pulses of two or more detectors arrive separated by less than a specified resolving time τ . To implement this comparison, the detector pulses are first narrowed in width and limited in height by a pulse shaper and limiter, followed by a coincidence element to determine the time overlap of the resulting pulses. A subsequent discriminator circuit makes the decision whether or not the pulses were separated by a time less than the resolving time.

The first electronic coincidence circuit, described in 1929 by Bothe,[1] operated on negative pulses of Geiger-counter detectors, shaped by RC differentiating networks, and limited by triodes operated at near-zero anode voltages. A tetrode, driven on the two grids by the limiter triodes, served as a coincidence element. The coincidences were registered by an electromechanical counter. The resolving time of the circuit was in the vicinity of 1 msec.

Detailed description of developments can be found in the excellent reviews available in the literature.[2-7] Attention will be focused here on circuits with short resolving times, suitable for operation at high counting rates.* Resolving times under 10 nanoseconds were achieved by Garwin[9] in 1950. The circuit (Fig. 1) operates on scintillation counters followed by photomultiplier tubes as detectors. The detector pulses are clipped to 8-nsec widths by shorted cables placed at the grids of the input limiter triodes. The anode currents are added on diode D1 ("Garwin diode"). When only one triode is cut off by a detector

* When counting rates are relatively low and long dead times are acceptable, time conversion techniques can be utilized. In a circuit described in Ref. 8, the detector pulses excite ringing circuits with different resonant frequencies and timing information is derived by the demodulation of the 3-MHz interference frequency. Resolving times of 0.2 nsec with dead times in the vicinity of 3 μsec were attained by this method.

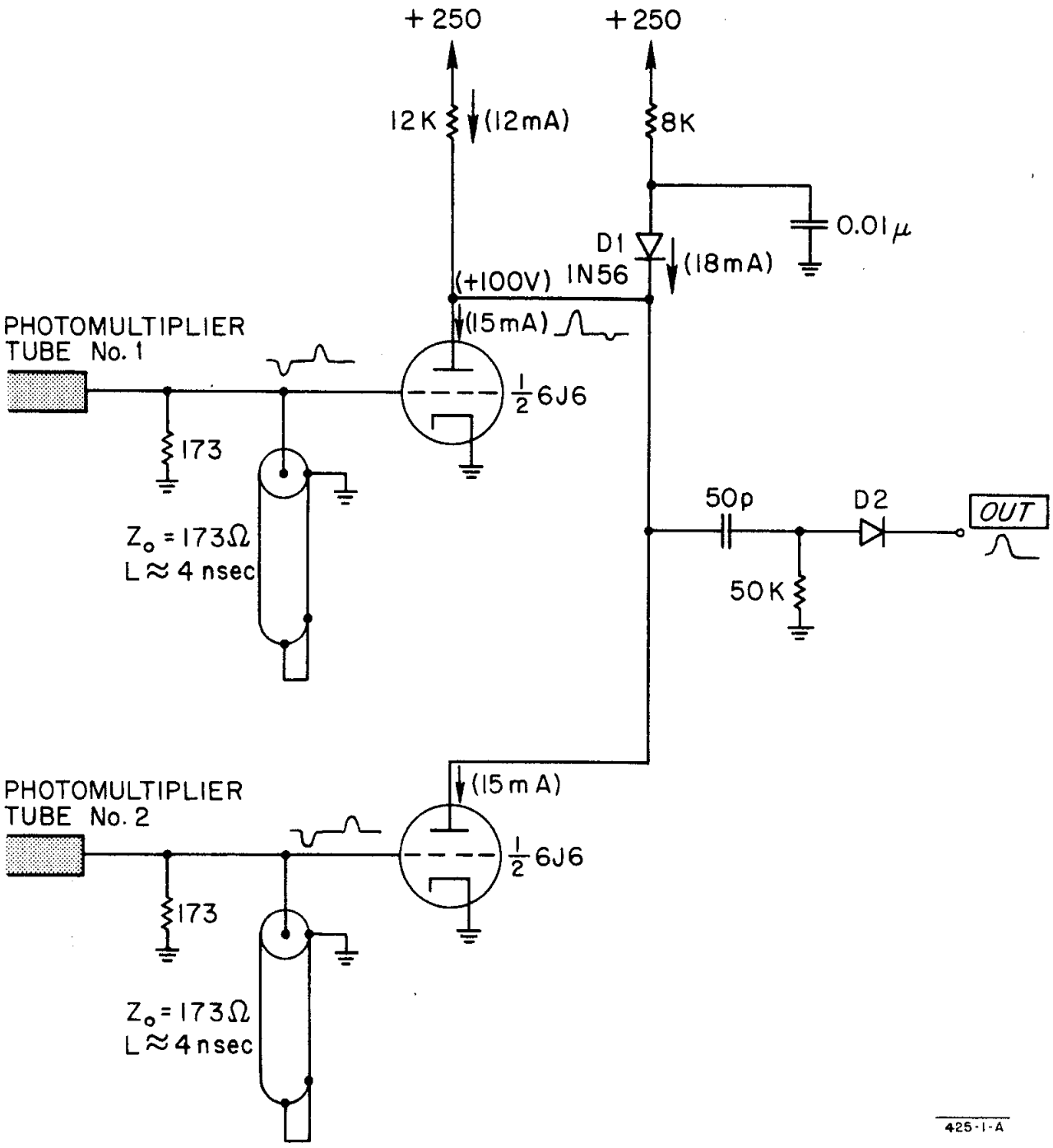

FIG. 1

COINCIDENCE CIRCUIT OF REF. 9.

pulse, the current in diode D1 drops from the quiescent 18 mA to about 3 mA, and a small (<1V) output voltage results. When both triodes are cut off simultaneously, diode D1 cuts off, the anode voltage starts to rise from 100 V toward 250 V, and a large output pulse results. The shortest attainable resolving time is limited primarily by the detector pulses, by the storage time of diode D1, and by stray capacitances.

In the circuit of Fig. 1, the positive part of the clipped grid signal turns on a large current in the triode and in diode D1. This results in a large excess charge stored in the diode, requiring a finite time to be swept out. If a second pulse arrives during this time -- a likely event at high counting rates -- it might be registered as a coincidence. For this reason, the clipping line was moved from the grids to the anode by Bell, Graham, and Petch[10] (Fig. 2).

With the advent of high-energy accelerators, satisfactory operation at high counting rates became very important. A circuit of Wenzel[11] designed for operation at high rates is shown in Fig. 3. Here the detectors are direct coupled to the circuit and the pulses are kept short by low (125-Ω) impedances at the inputs. Mismatches in the termination of the input cables may result in small positive overshoots which are transmitted to the anodes as negative pulses; these, however, are isolated by diodes and do not result in feedthrough of single input signals. Resolving times of better than 2 nsec were measured at counting rates of up to 1 MHz.*

With the introduction of fast transistors in the late 1950s, several circuits started to utilize them.[12-20] A circuit of Ref. 17 is shown in Fig. 4. The input cables are terminated by a network containing a level restoring diode minimizing "pile-up" at high counting rates. The input limiters are difference

* 1 Hz ≡ 1 cps.

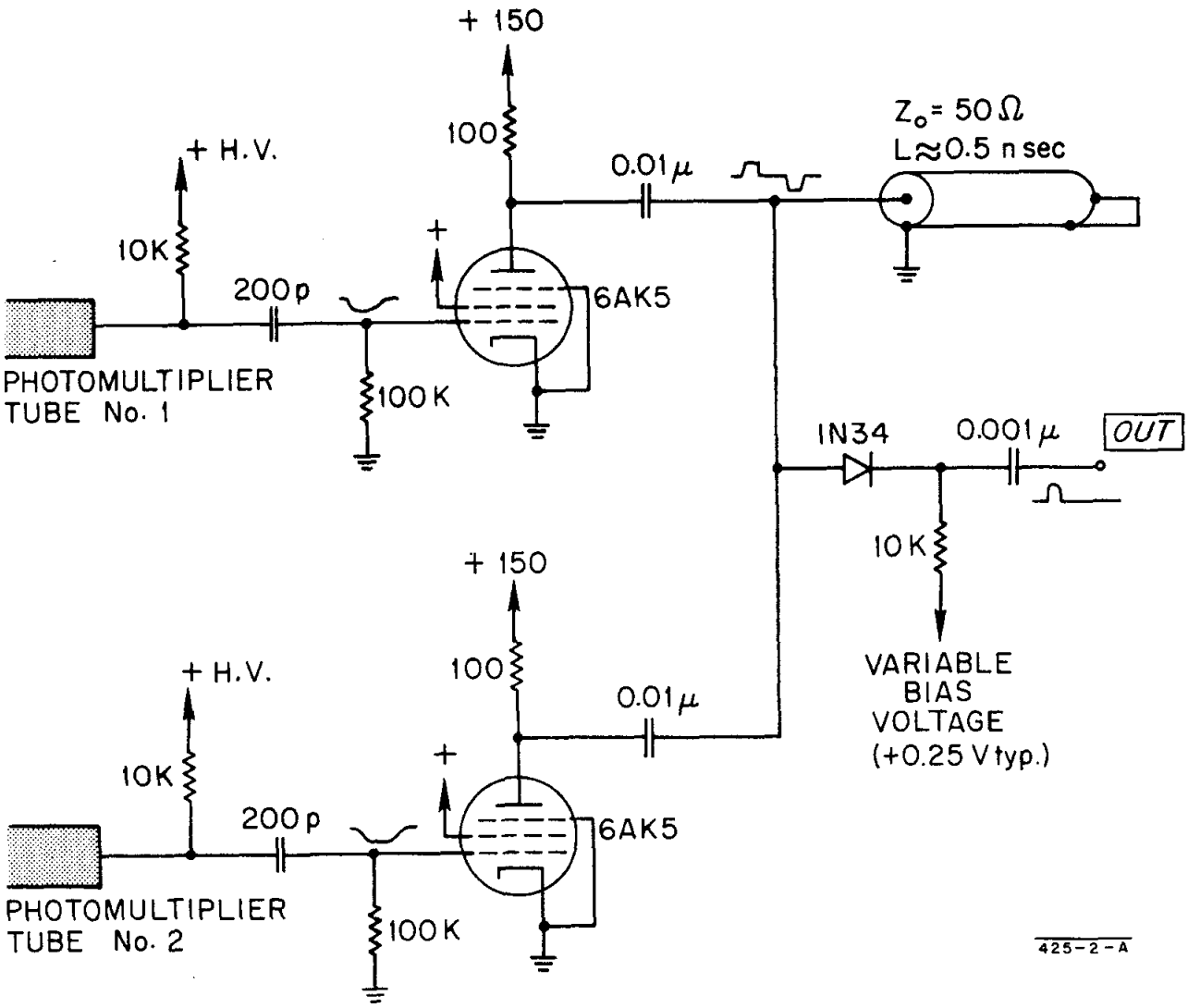

FIG. 2

COINCIDENCE CIRCUIT OF REF. 10.

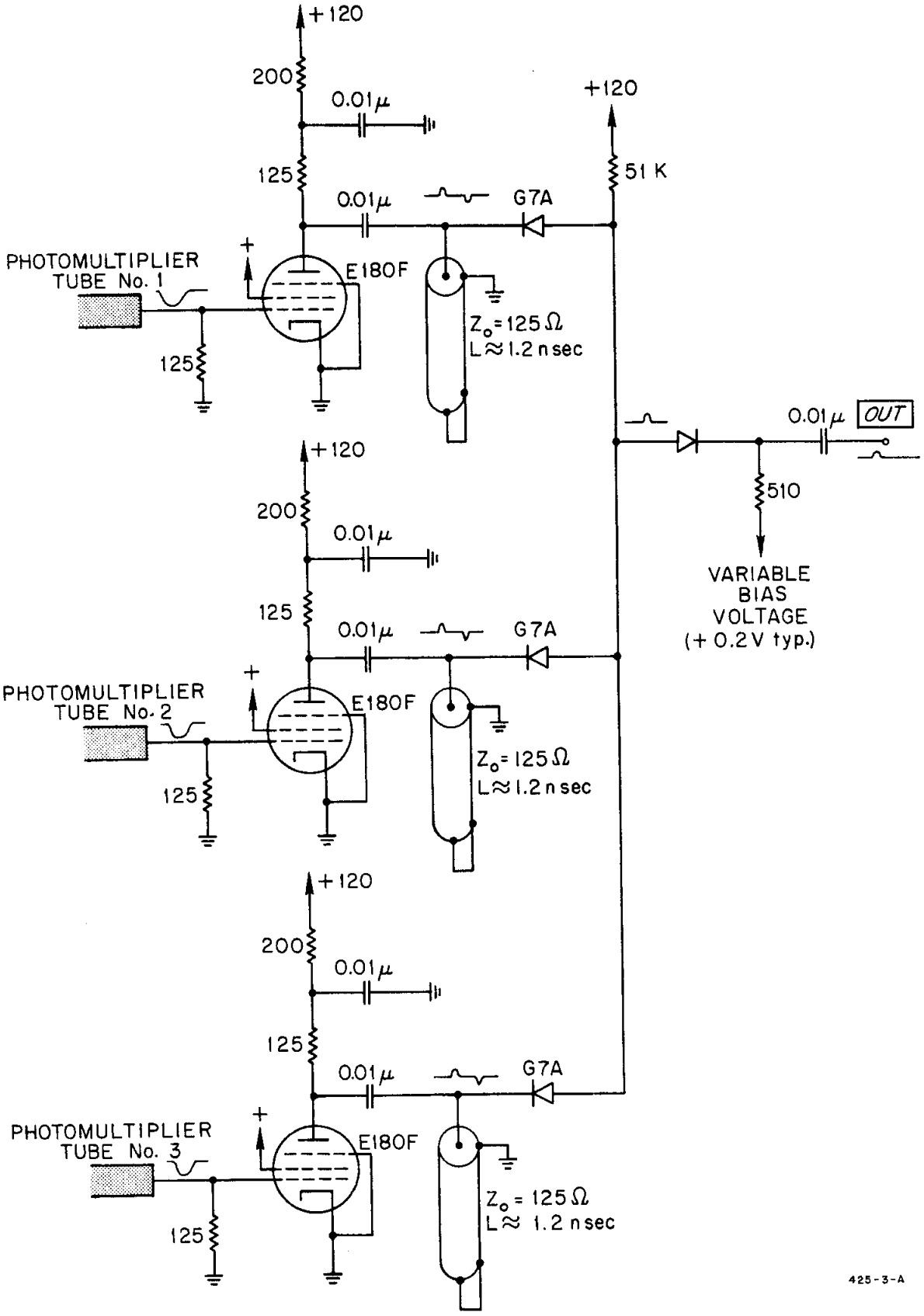

FIG. 3 COINCIDENCE CIRCUIT OF REF. 11.

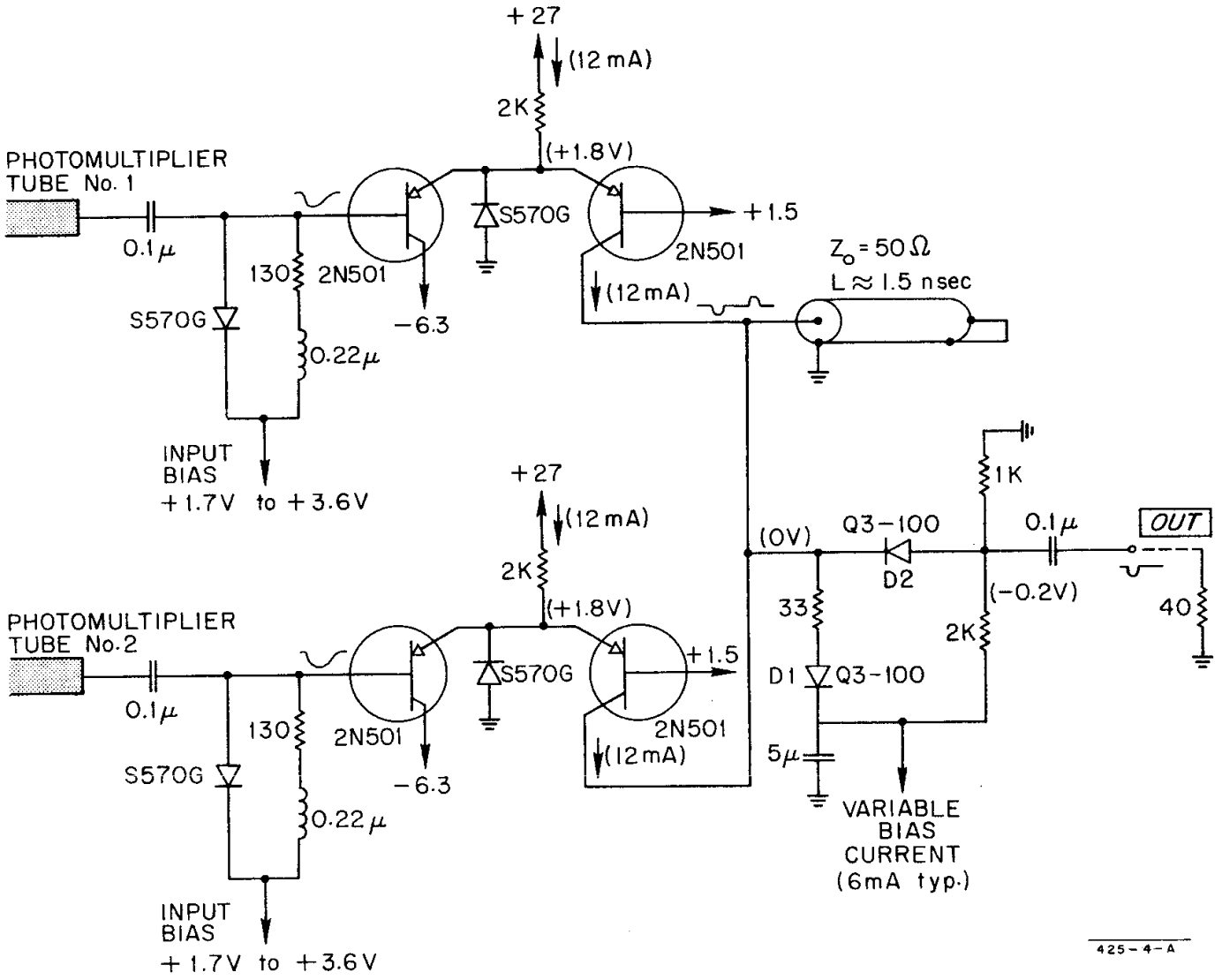

FIG. 4

COINCIDENCE CIRCUIT OF REF. 17.

amplifiers with the input-side transistors normally cut off; as a result, unlike in the circuit of Fig. 2, small positive signals at the input produce no detrimental effects. The currents of the difference-amplifiers are added on "Garwin-diode" D1. This diode is imbedded in a network providing an approximately 50-Ω impedance for the termination of the clipping line. Resolving times of better than 2 nsec were measured at counting rates of 1 MHz.

As fast tunnel diodes became available, many circuits were built using them.[21-35] Principal components of the input shaper and the coincidence element of one of these (Ref. 33) are shown in Fig. 5 and Fig. 6, respectively. Tunnel diode D1 provides limiting for unusually large input pulses. Transistors Q1 and Q2 in Fig. 5, comprise an input limiter supplying a current pulse to tunnel diode D2, resulting in transferring it from its quiescent bias point of near its peak current to its "high" state ($V > V_{valley}$). Transistors Q3, Q4, Q5 and Q6 reset D2 after a time L. The input impedance of the coincidence element of Fig. 6 terminates the 50-Ω cables connecting it to the preceding input shapers of Fig. 5. The coincidence element has four inputs, any number of which can be disabled (by means not shown in the figure). This system is capable of operating at resolving times in the vicinity of 3 nsec. Since it is directly coupled, there are no adverse "pile-up" effects at high counting rates, which rates are limited only by the minimum acceptable pulse spacing of 10 nsec.

II. COMPONENTS OF THE 0.3-NSEC COINCIDENCE CIRCUIT

The components of the system with a resolving time of 0.3 nsec are shown in Fig. 7. The 14-stage photomultiplier tubes* have anode pulse risetimes in the vicinity of 500 psec. In order to preserve this risetime, the connection

* Radio Corporation of America, C70045A developmental types.

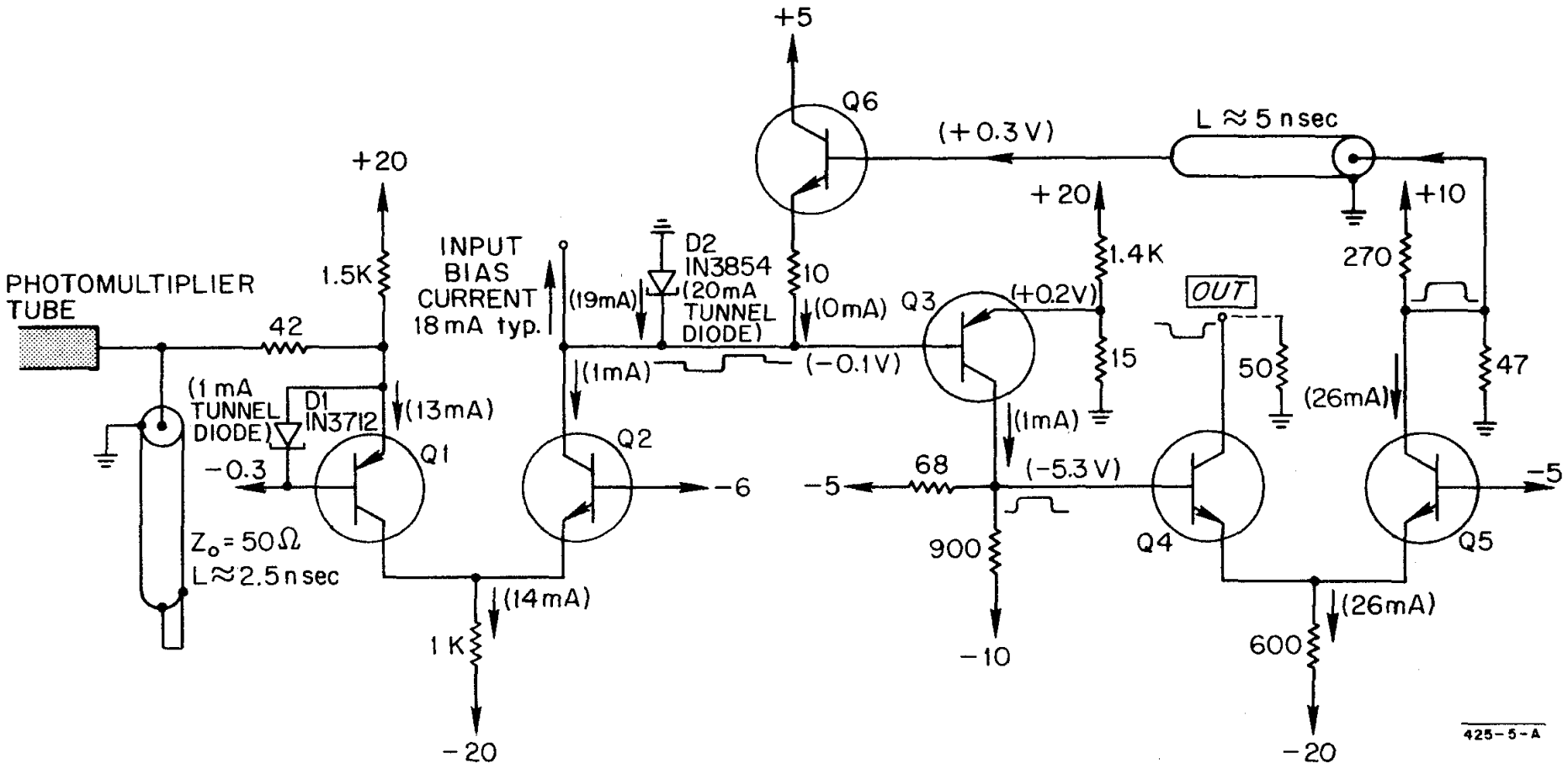

FIG. 5

PRINCIPAL COMPONENTS OF THE INPUT SHAPER OF REF. 33.

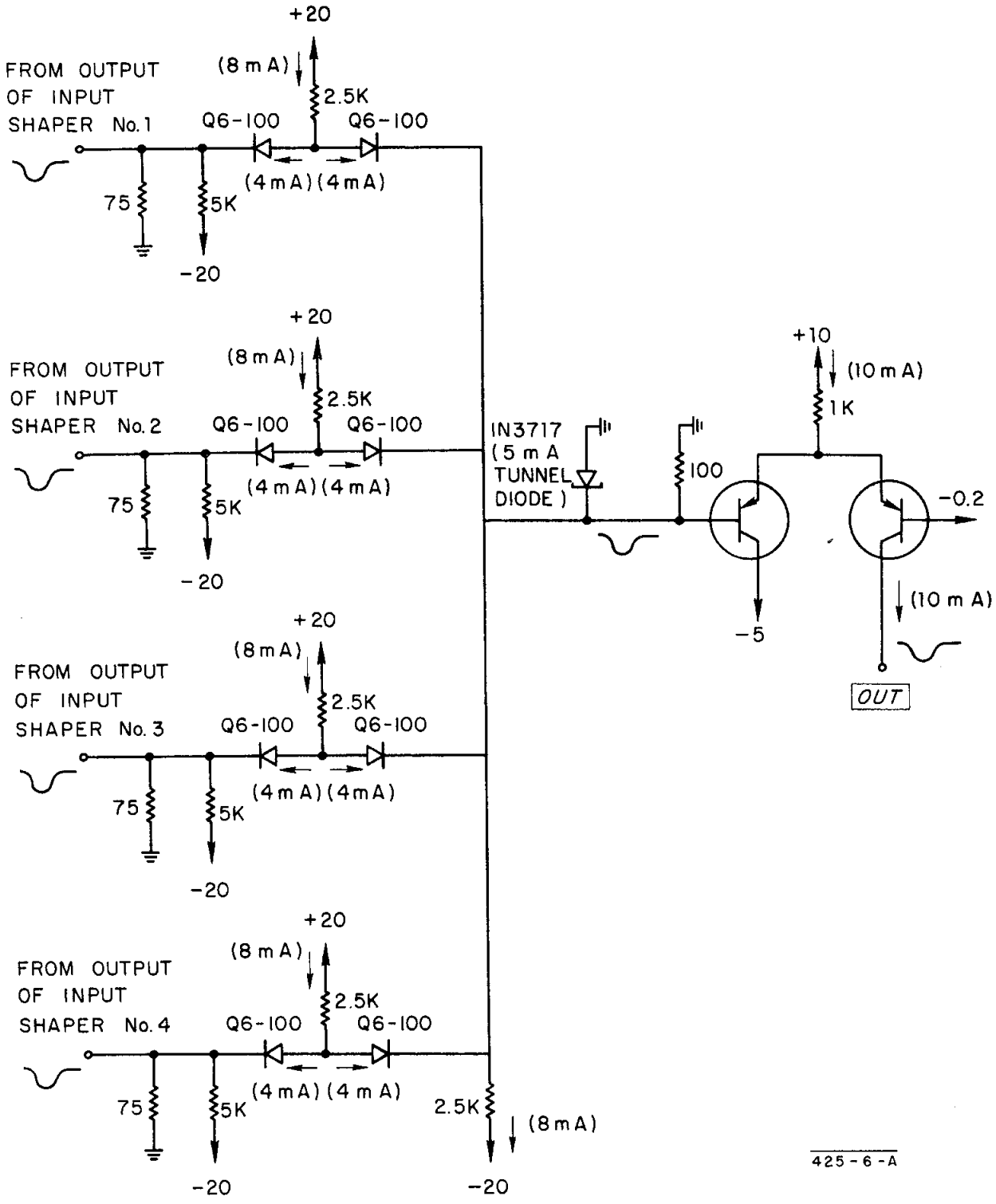

FIG. 6

PRINCIPAL COMPONENTS OF THE COINCIDENCE ELEMENT OF REF. .33.

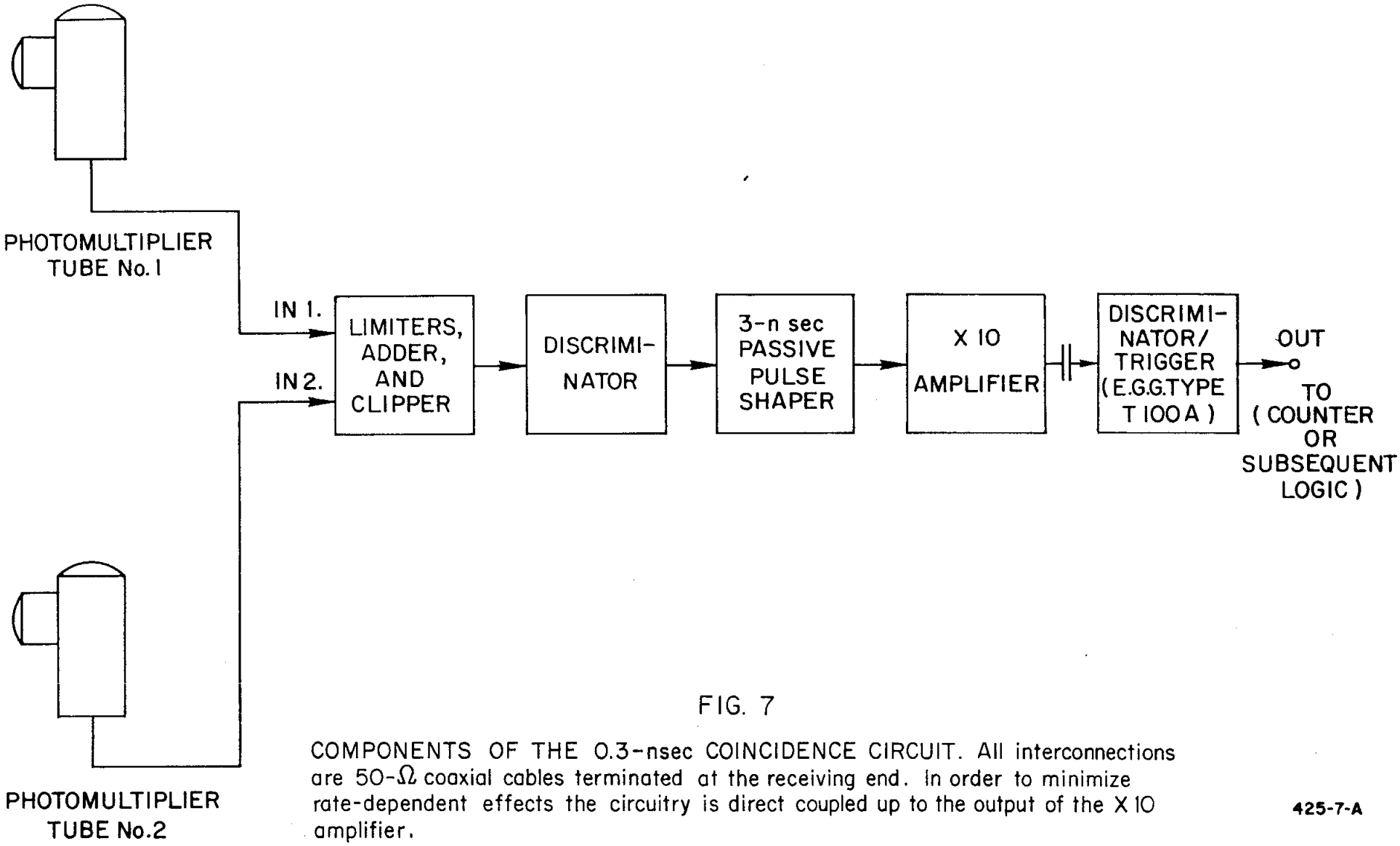

FIG. 7

COMPONENTS OF THE 0.3-nsec COINCIDENCE CIRCUIT. All interconnections are 50-Ω coaxial cables terminated at the receiving end. In order to minimize rate-dependent effects the circuitry is direct coupled up to the output of the X 10 amplifier.

425-7-A

to the anode is made via 50-Ω coaxial cable, which has to be terminated at the receiving end to avoid undesirable reflections.

The two photomultiplier tubes are followed by the input limiters shown in Fig. 8. These limiters are direct-coupled differential amplifiers insensitive to small positive signals on the input terminals. Negative pulses on input 1 and input 2 transfer the approximately 8-mA standing currents from input transistors Q1A and Q2A to output transistors Q1B and Q2B respectively. The collector currents of Q1B and Q2B are linearly added on a shorted clipping line of electrical length L. Typical input-voltage, collector-current, and output-voltage waveforms are shown in Fig. 9. When the leading edges of the input pulses are separated by a time more than 2L (a), or by 2L (b), the negative output pulse height does not exceed V_o. When the leading edges of the input pulses are separated by a time less than 2L (c), the negative output pulse height exceeds V_o.

The decision, whether the leading edges of the photomultiplier pulses are separated by less than 2L, or by more, is made by the discriminator of Fig. 10. When separation is more than 2L, the pulse from the limiter circuit is insufficient to drive the tunnel diode over its peak current, and a small output pulse will result. When separation is less than 2L, the tunnel diode is driven over its peak current into its "high" state, and a large ($V > V_{valley}$) output pulse will be obtained.

The output pulse of the discriminator is shaped to a critically damped 3-nsec wide pulse by the passive shaper of Fig. 11. When its output is terminated by 50-Ω, the shaper has an input impedance of 50-Ω and, for a delta function input, its output signal is of the form $t \cdot \exp(-t/\tau)$, with $\tau \approx 2$ nsec.

The signal is further processed to the input of a subsequent discriminator/trigger circuit through an amplification of 10 with a risetime of 2 nsec. The

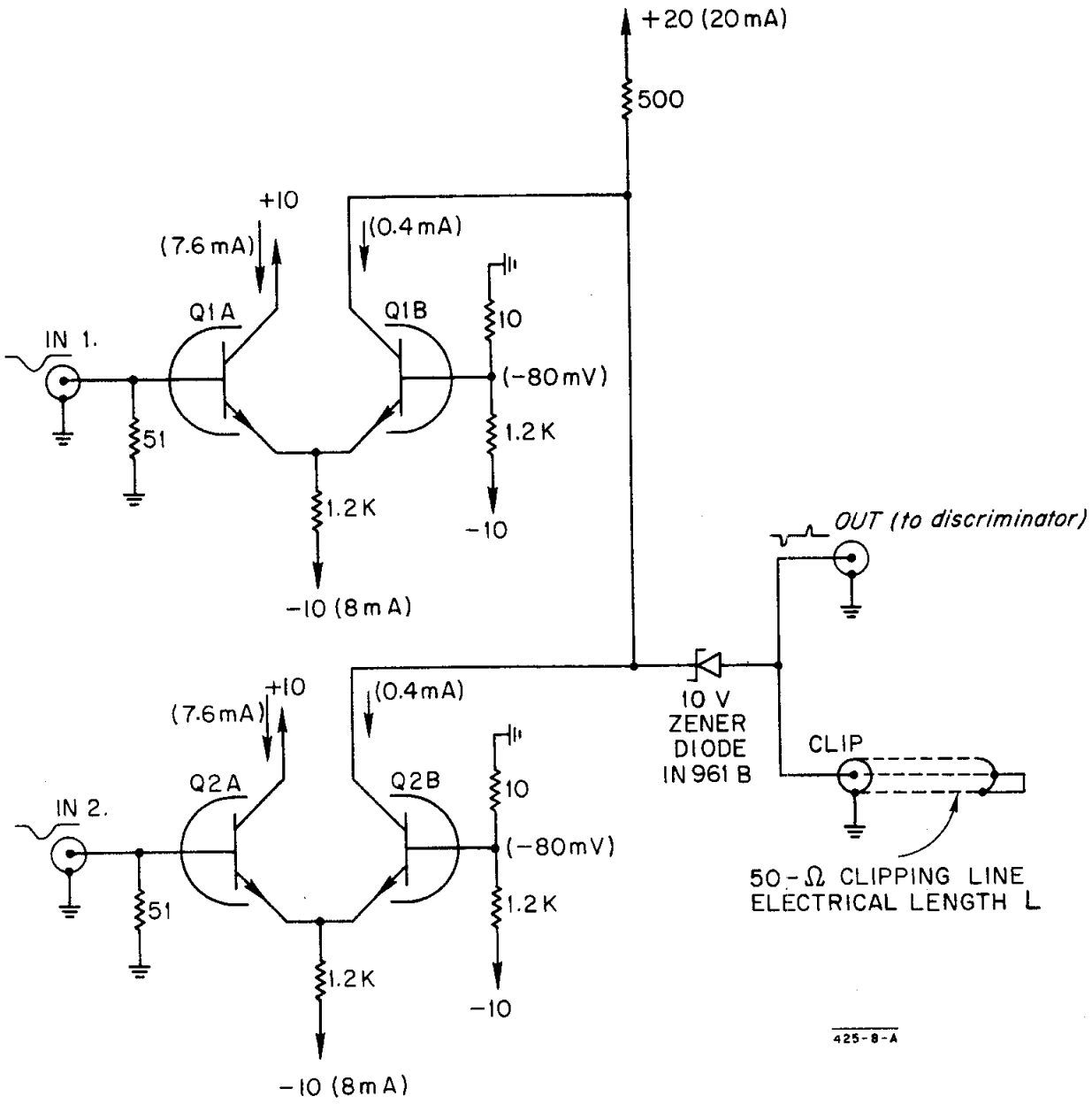

FIG. 8

INPUT LIMITER, ADDER, AND CLIPPER. SCHEMATIC DIAGRAM.
TRANSISTORS Q1 AND Q2 ARE MD1132F WITH β>150, OR SD519.

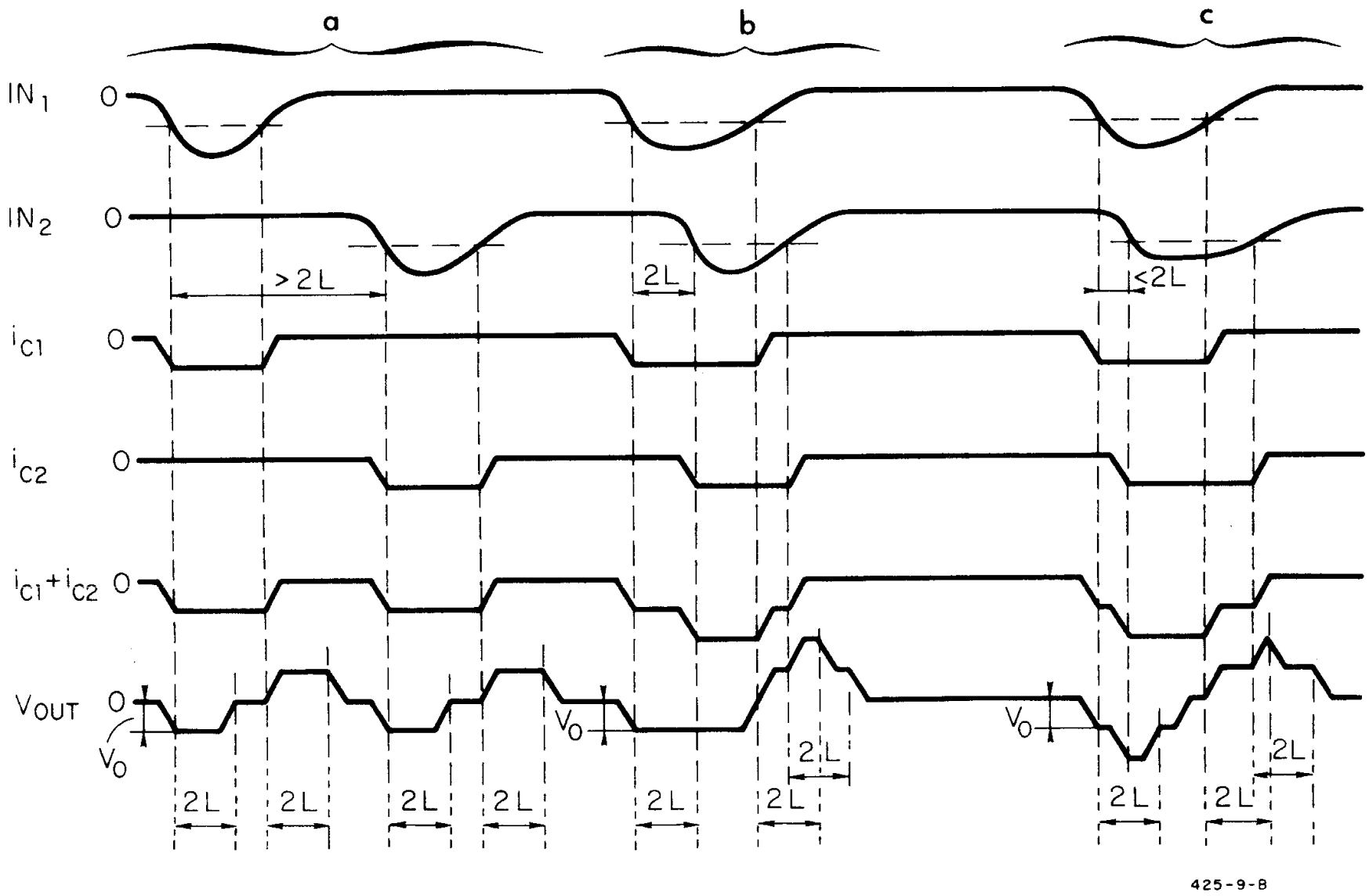

FIG. 9

INPUT LIMITER, ADDER, AND CLIPPER. IDEALIZED WAVEFORMS.

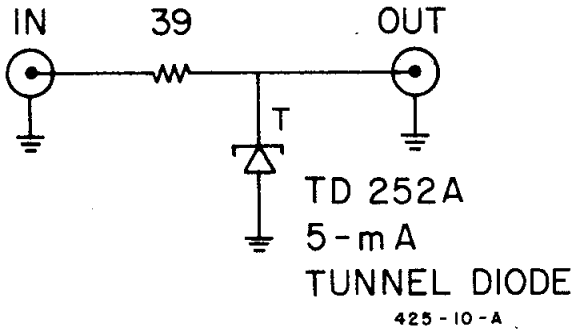

FIG. 10

DISCRIMINATOR. SCHEMATIC DIAGRAM.

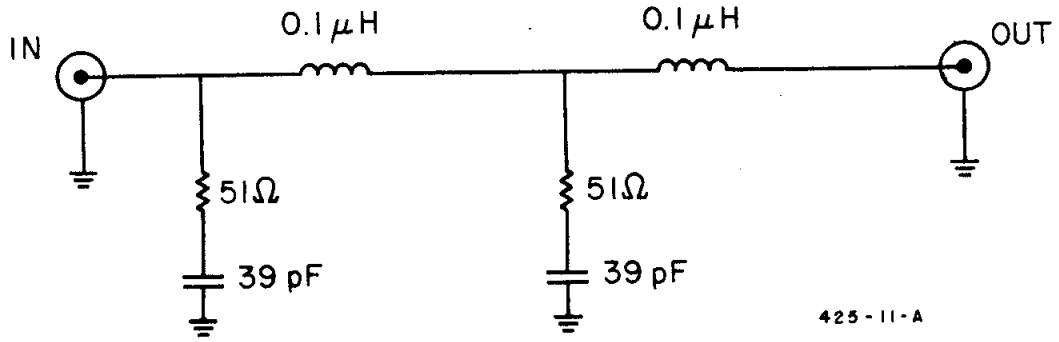

FIG. 11

3-nsec PULSE SHAPER. SCHEMATIC DIAGRAM.

discriminator/trigger circuit* has a threshold adjustable from -50 mV to -550 mV. The output pulse width W is variable from a minimum of 5 nsec; the maximum output pulse frequency is 1/(2 W).

In order to insure reliable operation at high rates, the circuit is direct coupled up to the input of the discriminator/trigger circuit. The output of the discriminator/trigger circuit is usually connected to logic circuits or directly to an accumulating counter.

III. PHOTOMULTIPLIER TUBES

The C70045A experimental photomultiplier tube was developed for the U. S. Atomic Energy Commission by the Radio Corporation of America.[37-40] The tube has a curved side-window cathode with a quantum efficiency in the vicinity of 20%.† A transit-time spread of less than 100 psec ($\sigma \approx 30$ psec) between a 3.8-cm diameter area of the photocathode and the first dynode is achieved by a three-element lens system. The single-photoelectron response of the tube has a $\sigma \approx 135$ psec. When operated with a Čerenkov detector having a small time spread, the output pulse width can be shorter than 1 nsec.

The maximum sensitivity of the photocathode is between wavelengths of 4000 A^{o} and 5000 A^{o} and it drops to relative values of 1% at about 2000 A^{o} and 6300 A^{o}.

---

* The circuit is similar to that of Fig. 5.

† The performance data is taken from Ref. 36.

IV. INPUT LIMITERS (Fig. 8)

A. Steady State Current Distribution

Under quiescent conditions, the bases of input transistors Q1A and Q2A are at zero voltage, and the bases of output transistors Q1B and Q2B are at -80 mV. The ratio of the emitter currents can be written as

$$\frac{I_E(Q1A)}{I_E(Q1B)} = \frac{I_E(Q2A)}{I_E(Q2B)} = \frac{\exp(qV_{EB}^A/kT) - 1}{\exp(qV_{EB}^B/kT) - 1} \approx \exp(q\Delta V_B/kT)$$

$$\approx \exp(80\text{ mV}/26\text{ mV}) \approx 22$$

The total available current is 8 mA, thus the standing current in the input transistor is 7.6 mA and in the output transistor it is 0.4 mA.*

If an input becomes more negative than -160 mV, the emitter current of the corresponding input transistor will be reduced below 0.4 mA and the remainder of the 8-mA available current will flow into the emitter of the output transistor.

The current gains of the transistors are higher than 150, thus the base currents required to maintain the standing currents are less than 8 mA/150 = 63 μA. This dc base current will be neglected in the subsequent analysis.

B. Transient Response for a Step Function Input

If a negative step function with a height exceeding 160 mV is entered at one of the inputs, the current will be transferred from the input transistor to the output transistor. The transfer time, and thus the output risetime, will depend on the parameters of the transistors and on the circuit. The transistors used in

* The maximum base offset voltage is specified as 5 mV, which may modify the current distribution by 0.1 mA. For a description of the dual transistors used here, see Ref. 41.

the limiters are type MF 1132 F with $\beta > 150$. This unit is a package of two individual transistors each similar to the type 2N918. The gain-bandwidth product of this transistor type as a function of collector current is shown in Fig. 12.[42] It can be seen that as the collector current I_c varies from 0.4 mA to 8 mA, the gain-bandwidth product f_T changes from 400 Mc to 950 Mc. Thus, the use of a lumped model[43] in this case is not advantageous, and a different approach is taken.

The difference between the values of the stored base charge at t = 0 and at $t = \infty$ can be written as

$$\Delta Q \equiv \left| Q_c(t = 0) - Q_c(t = \infty) \right| = \int_{0.4\ \text{mA}}^{8\ \text{mA}} \frac{di_c}{2\pi f_T} \qquad \text{(IV. 1)}$$

The integration was performed graphically using the values of f_T from Fig. 12. This resulted in a $\Delta Q = 1.5$ pCoul, corresponding to an "average" f_T of 800 Mc. Neglecting collector-base capacitance (≈ 1 pF), this ΔQ equals the total charge injected into the bases

$$\Delta Q = \int_0^\infty i_b\, dt \qquad \text{(IV. 2)}$$

where i_b is the current charging the bases. The magnitude of this current is zero at $t = \infty$ and a finite I_b at t = 0. As for the actual waveform, several approximations are possible. One possibility would be to assume a constant current I_b for a fixed time and zero afterwards; another possibility would assume a linearly decreasing current. In the following the approximation will be made that the current decreases exponentially from its initial value of I_b to zero with a time constant of τ_1, and that the transient part of the output current can be approximated as 7.6 mA $\left[1 - \exp(-t/\tau_1)\right]$. As a further simplification, it will be assumed that a voltage of -160 mV of the input step function is required to

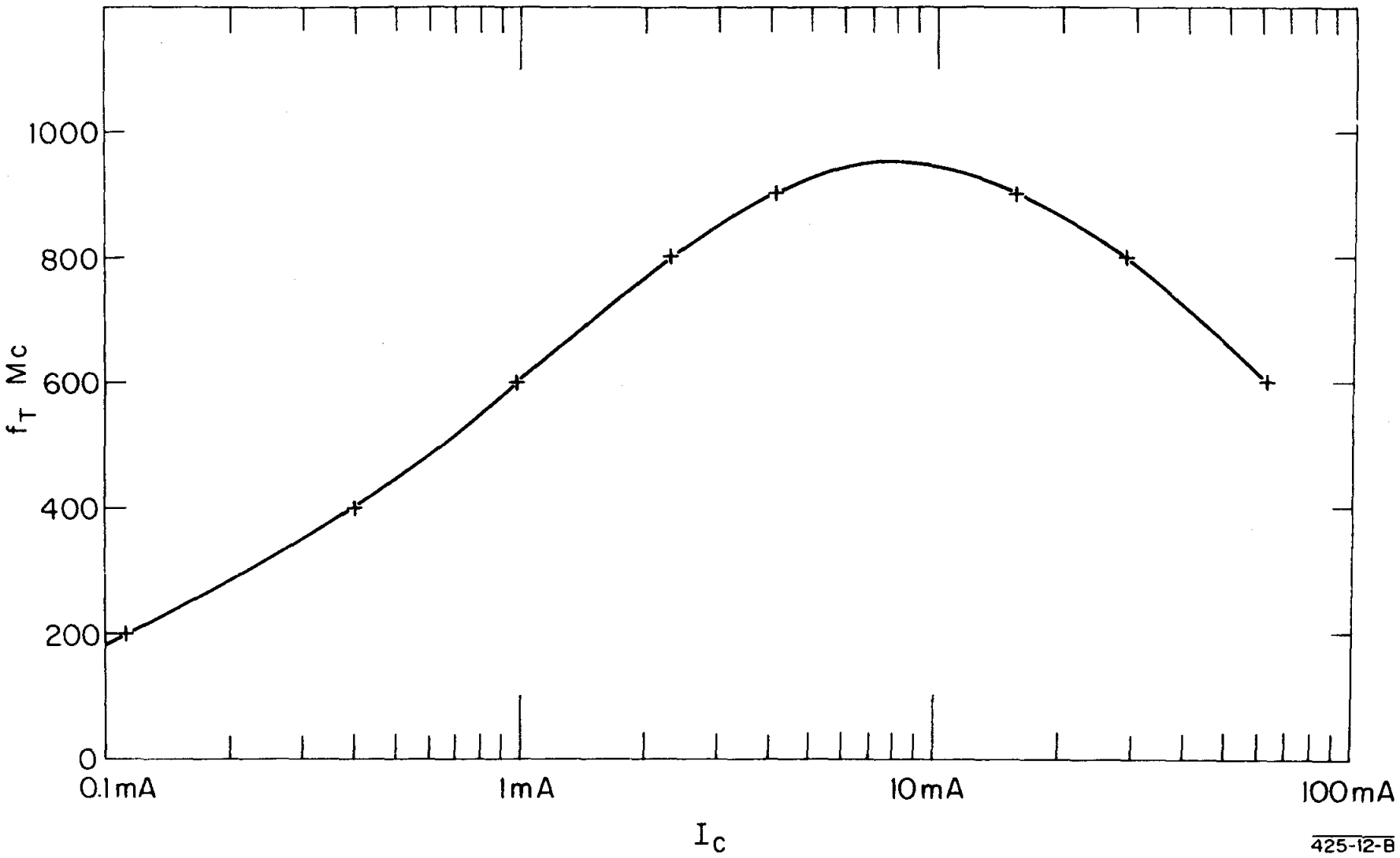

Fig. 12

TRANSISTOR 2N918. Gain-bandwidth product f_T as function of the collector current I_c at V_{ce} = 10V and at an ambient temperature of 25°C.

transfer the standing current, and the pulse height available to charge the bases is reduced by this amount. Thus the charging current at t = 0

$$I_b \equiv i_b(t = 0) = \frac{V_{in} - 0.16\ V}{Z_o/2 + 2r_b + R_b} = \frac{V_{in} - 0.16\ V}{75\Omega} \qquad \text{(IV.3)}$$

where V_{in} is the absolute value of the negative input step function, $Z_o = 50\,\Omega$ is the characteristic impedance of the input cable,* $r_b = 20\,\Omega$ is the ohmic base resistance of a transistor, and $R_b = 10\,\Omega$ is the external resistance in the base circuits of Q1B and Q2B. Combining Eqs. (IV.1), (IV.2), and (IV.3) one gets for τ_1

$$\tau_1 = \frac{\Delta Q}{I_b} = \frac{1.5\ \text{pCoul} \cdot 75\,\Omega}{V_{in} - 0.16\ V} = \frac{110\ \text{psec}}{V_{in} - 0.16\ V} \qquad \text{(IV.4)}$$

since ΔQ in Eq. (IV.2) is $I_b \tau_1$. An additional time constant of τ_c is located at the output:

$$\tau_c = 25\,\Omega \cdot 4\text{pF} = 100\ \text{psec} \qquad \text{(IV.5)}$$

Taking both τ_1 and τ_c into account, the output voltage can be written as

$$V_{out} = 190\ \text{mV} \cdot \mathcal{L}^{-1}\left[\frac{1}{p(1 + p\tau_1)(1 + p\tau_c)}\right] \qquad \text{(IV.6)}$$

Output voltage waveforms for various values of V_{in} were computed from Eq. (IV.6), and the 10% to 90% risetimes and the delays at the 50% point were determined graphically. As a result of the finite dimensions of the circuit, 0.5 nsec ($\doteq$ 15 cm) was added to the computed delay values.

The risetimes and delays thus determined are shown in Fig. 13 together

* A $Z_o/2$ appears in Eq. IV.3 because the cable is terminated by Z_o.

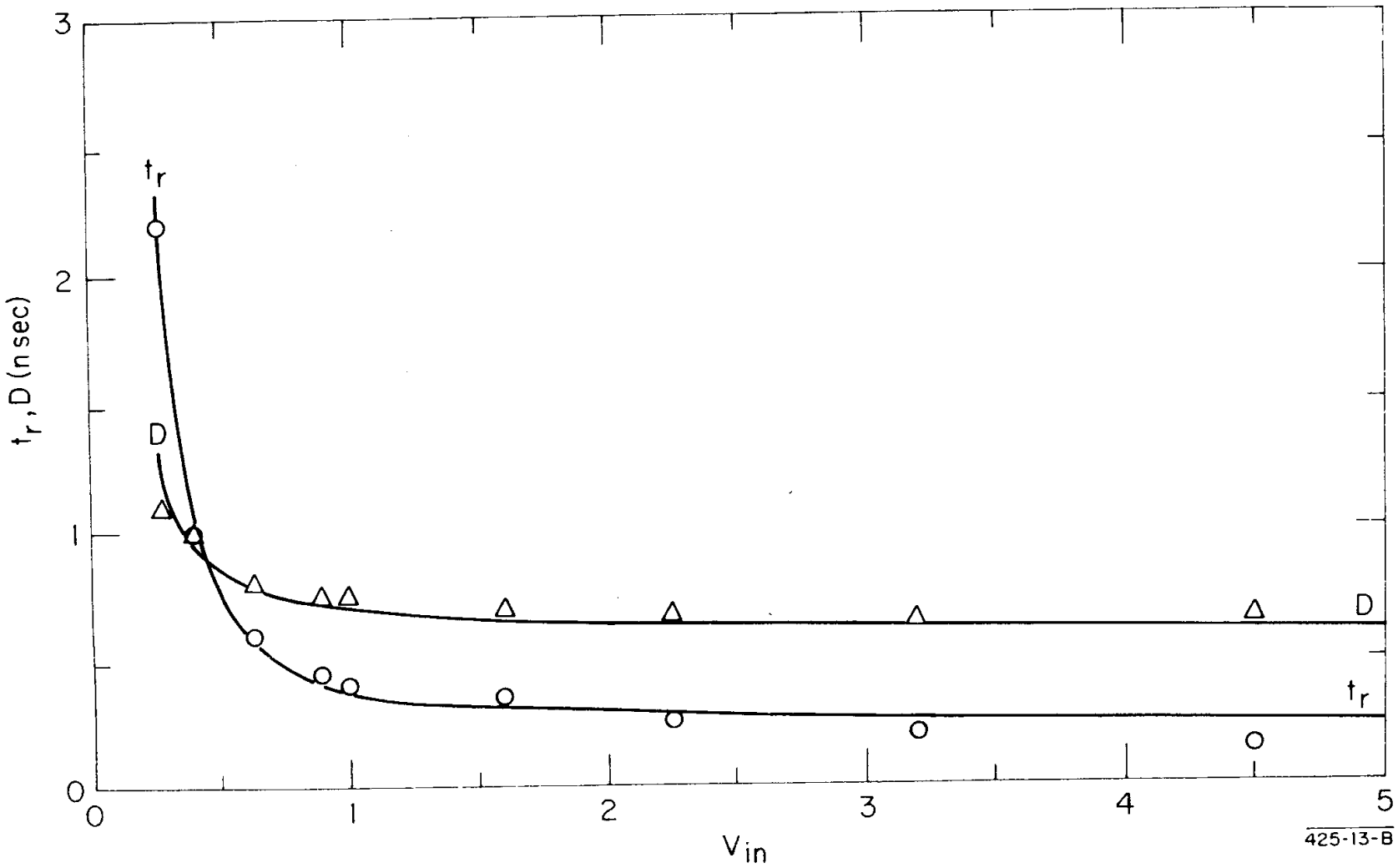

Fig. 13

INPUT LIMITER. 10% to 90% risetime t_r, and delay at the 50% point D, as a function of the input pulse height. The curves are obtained from (IV.6) with (IV.4) and (IV.5); 0.5 nsec was added to the computed delays to take into account the finite size of the circuit. Measured values of the risetime are denoted by O, measured delays by Δ.

with results of measurements performed with the test setup of Fig. 14. The measured data were not corrected for the risetime of the oscilloscope, since a significant overshoot and ringing (20% at $V_{in} = -1$ V) is present on the output, and this makes simple correction methods inaccurate.[44] The source of the overshoot and ringing is likely to be stray inductances.* An additional imperfection of the output signal is present in the form of a feedthrough from the input to the output consistent with a feedthrough capacitance of 0.1 pF. The output waveform for a step function input of -1 V is shown in Fig. 15.

C. Transient Response for 1-nsec-risetime Input

In order to obtain information on the properties of the limiter for input pulses with risetimes comparable to the pulses of the photomultiplier tubes, additional measurements were performed using slowed input pulses. The pulses of the mercury pulse generator were shaped by the network of Fig. 16 to a voltage of the form $V_{in}[1 - \exp(-t/0.4\ \text{nsec})]$. Results of measurements using this as an input pulse are shown in Fig. 17. It can be seen by comparison with Fig. 13 that for $V_{in} > 1.5$ V the performance of the limiter is not significantly deteriorated by the slower risetime of the input pulse.†

* A stray inductance of $(25\Omega)^2 \cdot 4\text{pF} = 2.5$ nH is sufficient to account for the overshoot and ringing observed.

† The maximum input pulse height is limited by the 5-V zener breakdown voltage of the base-emitter junction. If this input pulse height is exceeded, reflections will occur on the input cable.

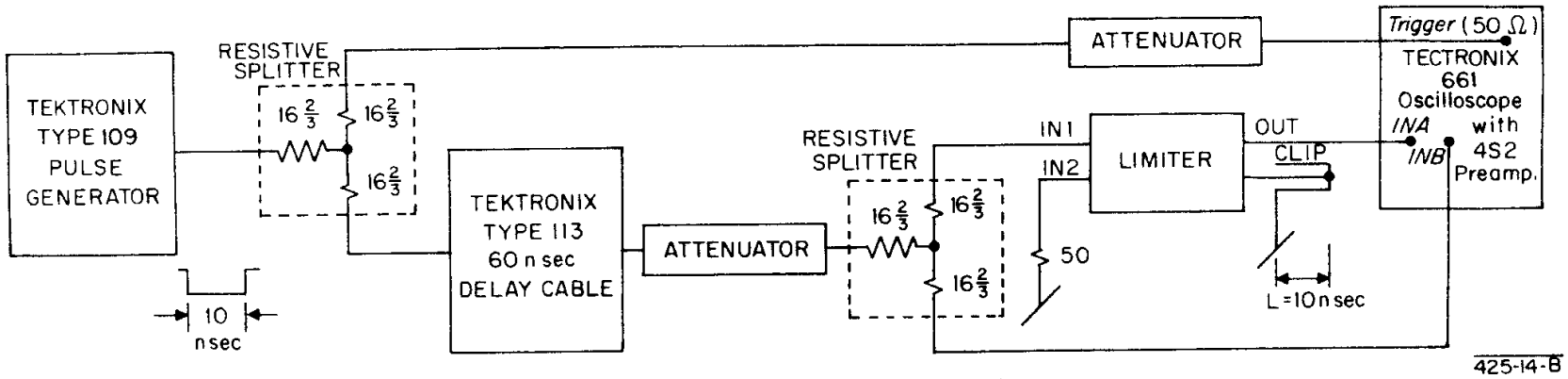

FIG. 14

TEST SETUP FOR THE MEASUREMENT OF THE TRANSIENT RESPONSE OF THE INPUT LIMITER.

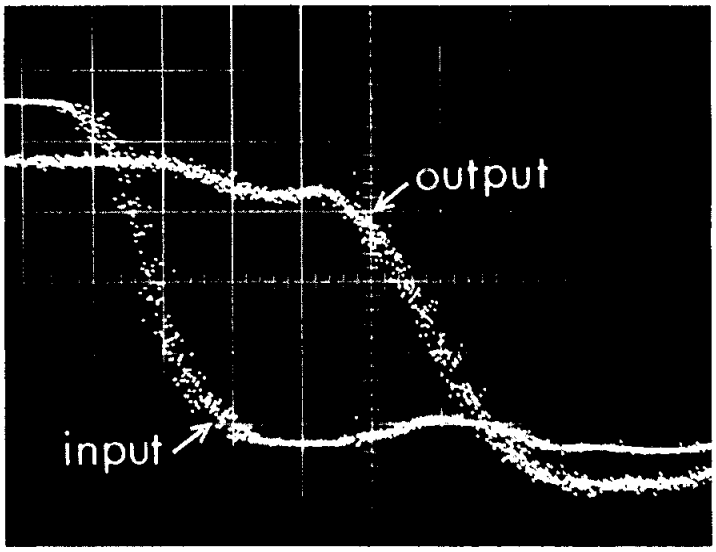

Fig. 15

INPUT LIMITER. INPUT AND OUTPUT WAVEFORMS FOR A -1V INPUT PULSE. Sweep Speed: 0.2 nsec/cm; Sensitivity: Input: 200 mV/cm, Output: 50 mV/cm.

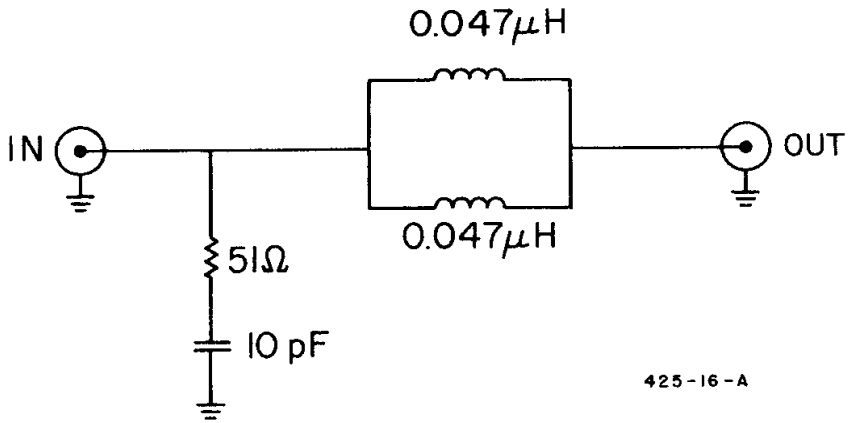

FIG. 16

0.4-nsec PULSE SHAPER. SCHEMATIC DIAGRAM.

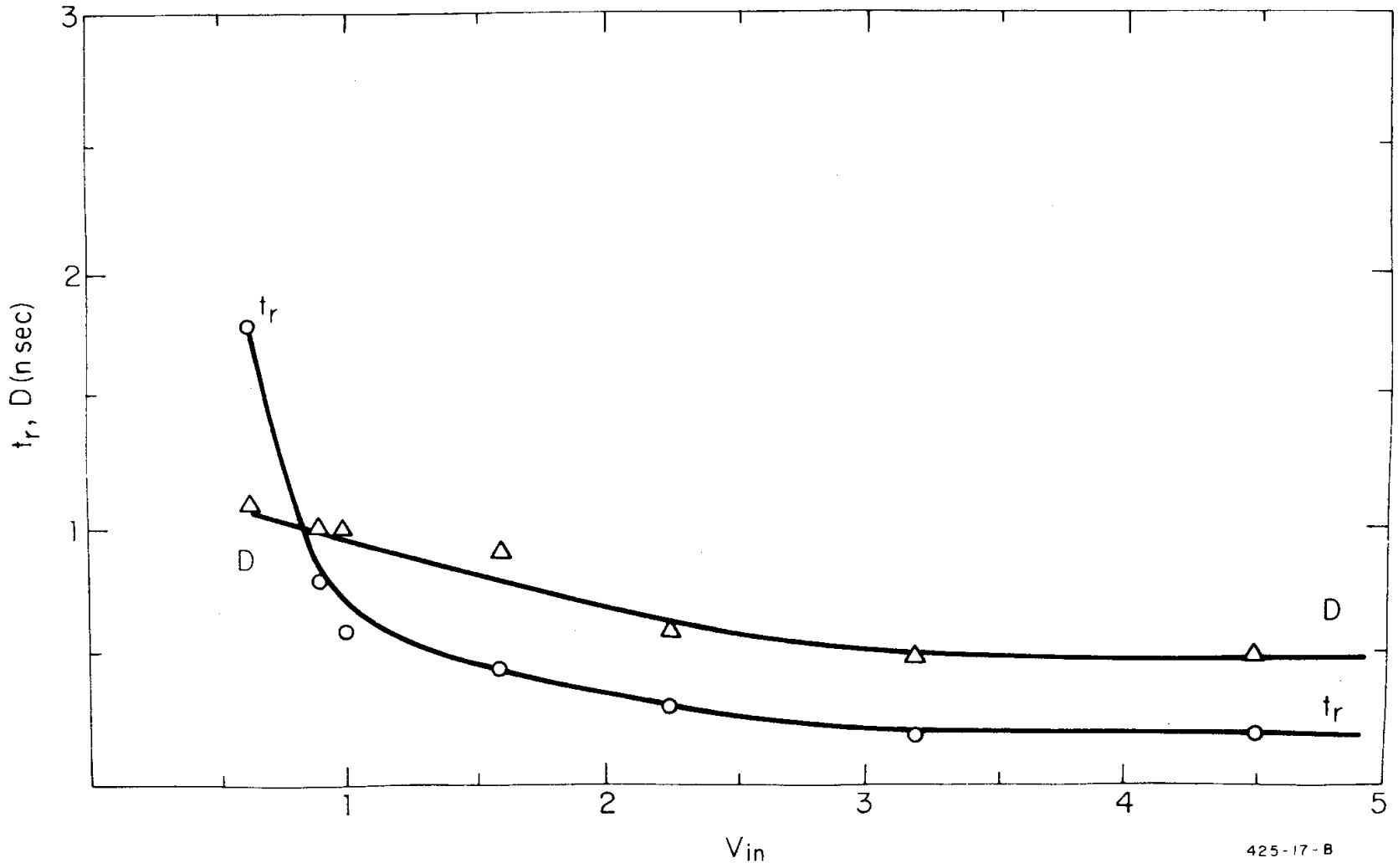

FIG. 17

INPUT LIMITER. 10% to 90% risetime t_r, and the delay at the 50% point D, as function of input pulse height for input pulses of the form V_0 [1-exp(-t/0.4 nsec)]. Curves represent fits to the measured points.

V. DISCRIMINATOR (Fig. 10)

In order to distinguish between coincident and non-coincident input pulses, the limiters are followed by a tunnel diode discriminator circuit. The qualitative features of the dc voltage-current characteristics of a tunnel diode are shown in Fig. 18. The initial operating point is at a voltage V_i and a current I_i. If the current is increased beyond I_p, the device switches to its high state ($V > V_v$). If no parasitic elements were present, this switching would be instantaneous; due to the capacitance and the inductance associated with the diode, however, switching requires a finite time. In order to investigate the switching process, the dc characteristics will be represented by a current generator i_s in parallel with a source impedance R (Fig. 19). The capacitance C includes that of the diode, plus any stray capacitance present; stray inductances are neglected.

In the particular circuit configuration used (see Figs. 8 and 10) for times less than 2L, $i_s = (i_{c1} + i_{c2})\, 50\,\Omega / (50\Omega + 40\Omega) = 0.55\,(i_{c1} + i_{c2})$, and $R = 50\Omega \cdot 90\Omega / (50\Omega + 90\Omega) = 32\Omega$, where $i_{c1} + i_{c2}$ is the sum of the collector currents. The capacitance of the TD252A tunnel diode is approximately 0.6 pF[45] and a value of 1 pF will be used for C.

A. Transient Response

If a single (non-coincident) input pulse enters the coincidence circuit, a tunnel diode current of $i_s = (i_{c1} + i_{c2}) \times 0.55 = -7.6\text{ mA} \times 0.55 = -4.2\text{ mA}$ will result. From the dc characteristics it can be concluded that approximately -3.4 mA of this current will flow into the tunnel diode and -0.8 mA will flow into R, and a voltage of -40 mV will be established. The time required to reach this equilibrium is in the vicinity of $1\text{ pF} \cdot 40\text{ mV}/4.2\text{ mA} \approx 10$ psec; in the following considerations this time will be neglected.

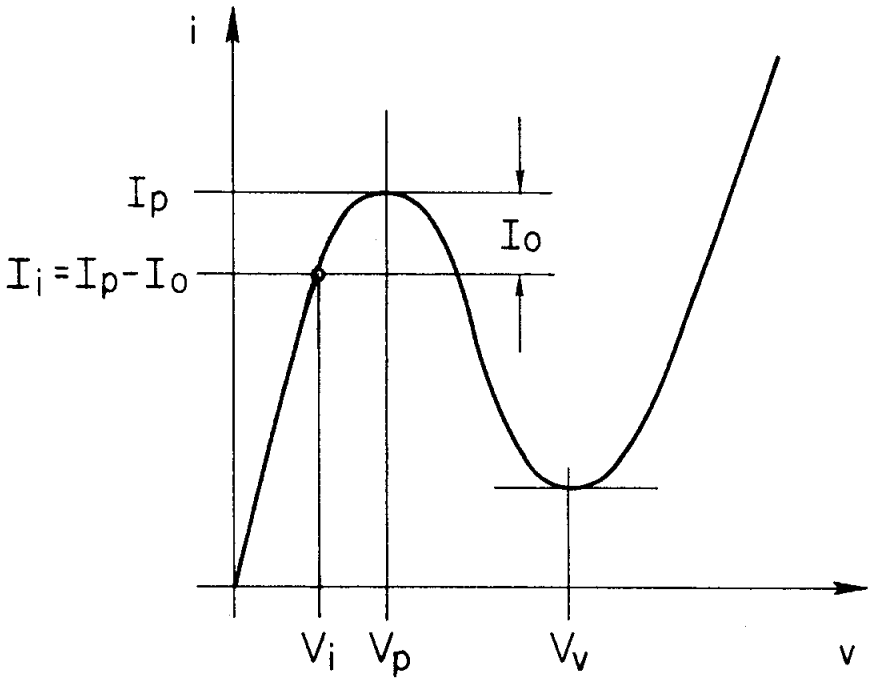

(a)

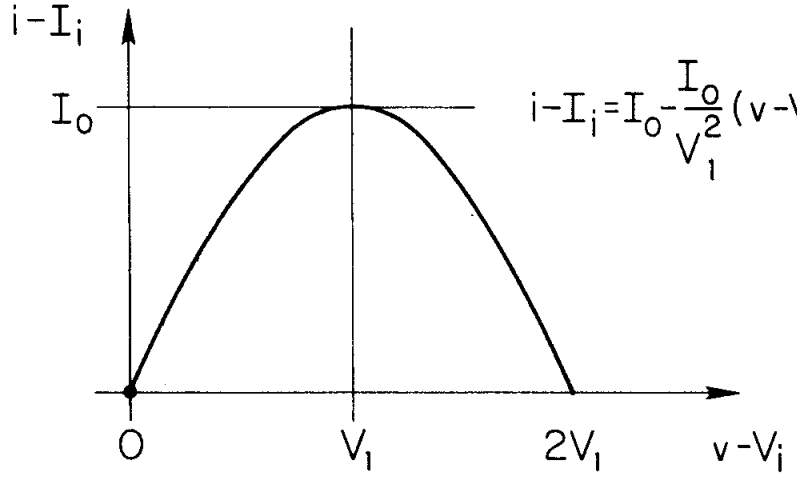

$$i-I_i=I_o-\frac{I_o}{V_1^2}(v-V_1)^2=2I_o\left(\frac{v}{V_1}\right)-I_o\left(\frac{v}{V_1}\right)^2$$

(b)

425-18-A

FIG. 18

TUNNEL DIODE dc CHARACTERISTICS (a), AND APPROXIMATION IN THE VICINITY OF V_p (b).

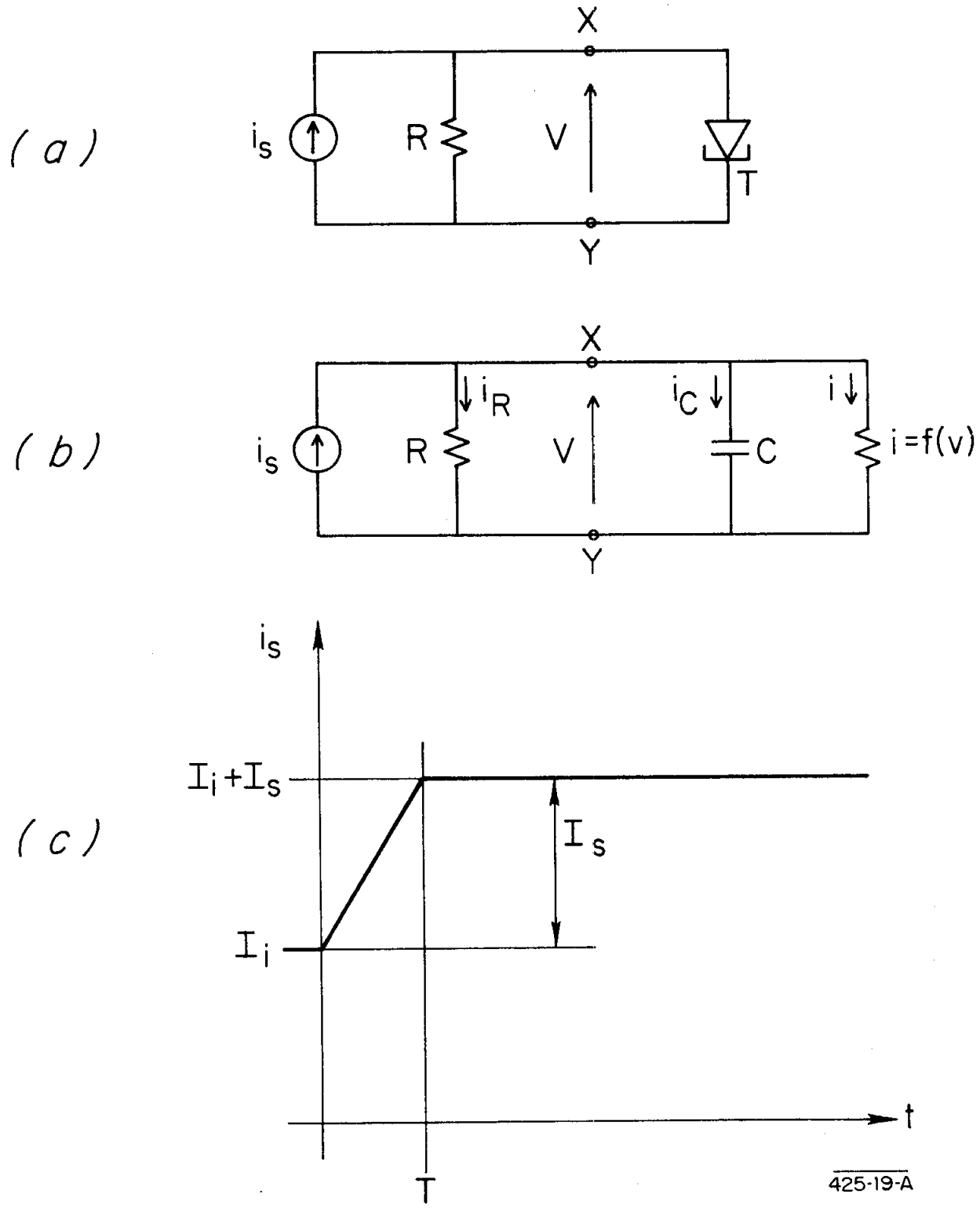

FIG. 19

TUNNEL DIODE CIRCUITRY (a), EQUIVALENT CIRCUIT (b), AND WAVEFORM OF I_s (c).

Let it be assumed next that, in addition to the input pulse on one of the inputs, a pulse will enter the other input. If the time difference between the two pulses exceeds 2L, the tunnel diode will make two excursions from v = 0 to v = -40 mV (Cf. Fig. 9). If the time difference is, however, less than 2L, following the arrival of the second pulse, the tunnel diode may switch from its "initial" -40 mV state to its high state.

In order to investigate this transition, the source current i_s will be approximated by the waveform of Fig. 19c. In general, the switching will begin at t = 0 and will be completed in a time shorter than, or longer than, or equal to T. Two limiting cases can be distinguished. The first one is when the switching is relatively slow and T is negligible with respect to the time required for the switching. This case, where the input signal can be treated as a step function, has been analyzed in the literature.[46, 47] The other extreme is when the switching is relatively fast, and is essentially completed within time T. It will be assumed that the second limiting case is a reasonable approximation; this assumption will be verified later.

For node X in Fig. 19b and for $t < T$, we can write

$$i_s = I_i + kt = i_R + i_c + i$$

with

$$k = I_s/T,\ i_R = v/R,\ i_c = C \cdot dv/dt,$$

and (from Fig. 18b)

$$i = I_i + 2I_o(v/V_1) - I_o(v/V_1)^2$$

the result is

$$C \cdot dv/dt - I_o(v/V_1)^2 + 2I_o(v/V_1) + v/R - kt = 0 \qquad (V.1)$$

With the introduction of normalized parameters

$S \equiv 1 + V_1/(2RI_o)$ as a measure of the source inductance,

$y \equiv v/(V_1 \cdot S)$ as a normalized voltage,

$x \equiv I_o St/(CV_1)$ as a measure of time, and

$A \equiv kCV_1/(I_o^2 \cdot S^3)$ as measure of the slope of i_s;

equation (V.2) becomes

$$dy/dx - y^2 + 2y - Ax = 0 \qquad (V.2)$$

This nonlinear differential equation* has been solved for an initial condition of $y(x = 0) = 0$ by the use of a digital computer.** The computer program is shown in Table I.† This program was followed by values of A and of increment DEL. Values of y as a function of Ax with A as parameter are shown in Fig. 20. For large A, $y \to Ax^2/2$; for small A, $y \to 1 - (1 - Ax)^{\frac{1}{2}}$.

TABLE I.

```
1046  ALGOL 19     10000 SLAC (AB)       343  DIFF EQ
        STANFORD B5500 ALGOL --  5/7/65 VERSION          228/65
BEGIN REAL A, YPRIME, Y, X, DEL;
FORMAT  F2(" A IS  ", F10.3),
FS ("          X          Y                YPRIME  ", "DEL IS", F10.5);
LABEL L1, L2, L3, QUIT;
L1: READ (      A) [QUIT]; WRITE (F2, A); X ←O.; Y←O.; YPRIME ←O.;
READ (     DEL); WRITE (F5, DEL) ;
L2:  X←X+DEL; Y←Y+YPRIME × DEL;  YPRIME ←Y×Y + A×X -2.×Y;
WRITE ( X, Y, YPRIME); IF ( Y ≥ 10.001 ) THEN GO TO L3 ELSE GO TO L2;
L3: GO TO L1;
QUIT:  END.
```

* The choice of variables, whereby y is zero initially, and y = 1, corresponding to zero damping ($\alpha = 0$), is by no means unique.

** The Burroughs B5500 computer of Stanford University was used via the SLAC data link.

† The program was written by M. Kreisler.

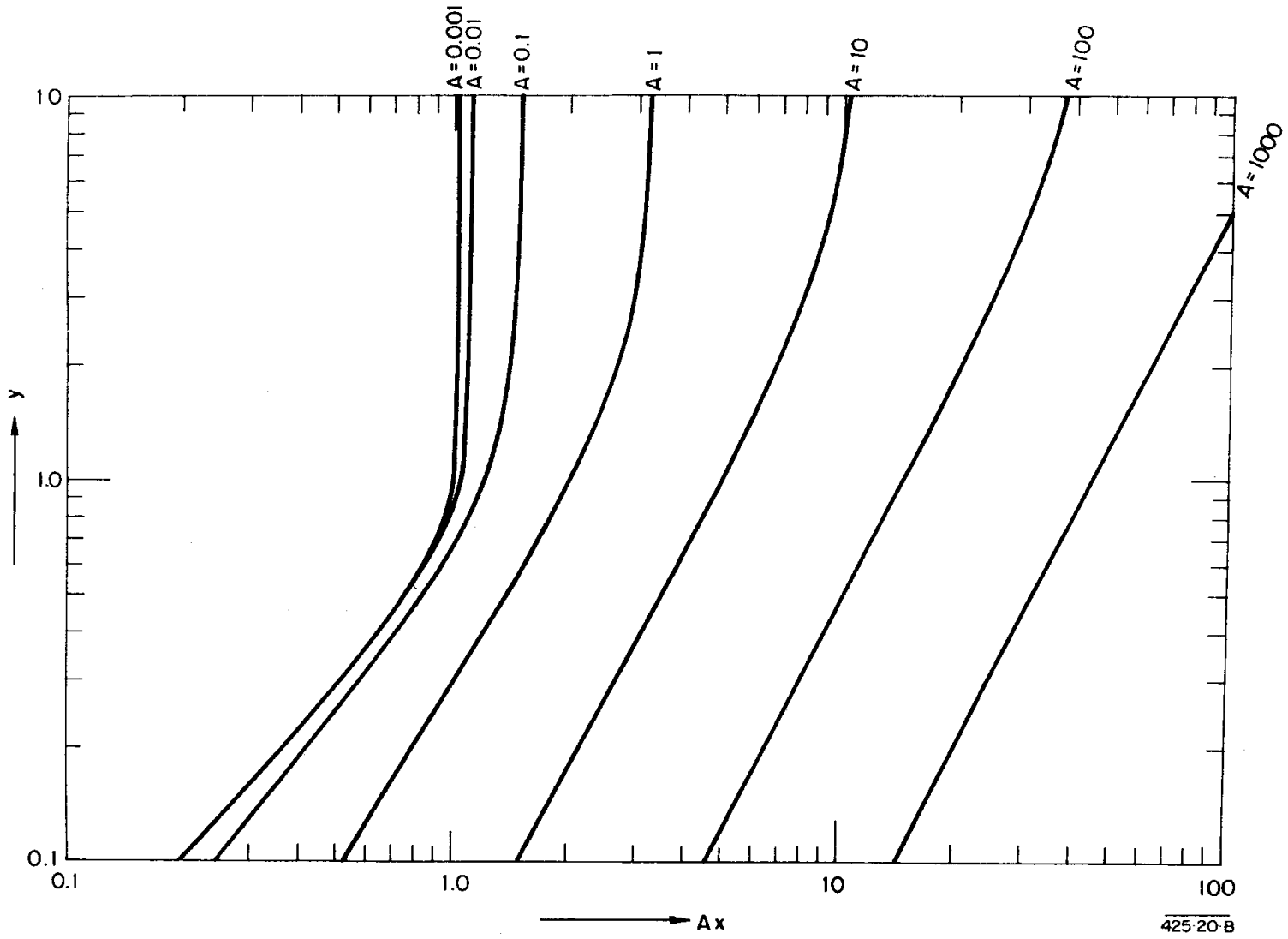

Fig. 20

NORMALIZED VOLTAGE y AS FUNCTION OF NORMALIZED TIME Ax WITH A AS PARAMETER, AS COMPUTED NUMERICALLY.

B. Tunnel Diode Triggering Jitter

If the normalized voltage y reaches a value of 1, a transition to the high state of the tunnel diode may take place. For $y < 1$ the damping rate α is negative; for $y > 1$ it is positive. The current flowing into the tunnel diode is a superposition of a fraction of I_s and of noise current. The actual time of reaching $y = 1$ (corresponding to $\alpha = o$) is thus determined by the noise, hence a time jitter results.[48] For a regenerative circuit this jitter has been computed as[49]

$$\tau_j \approx 1.22(d\alpha/dt)^{-\frac{1}{2}}_{\alpha=o} \qquad (V.3)$$

It can be seen that the time jitter, although a result of the presence of noise, is independent of the noise level.

The damping rate α can be written as

$$\alpha = -1/RC = -C^{-1} \cdot di/dv$$

and

$$d\alpha/dt = (d\alpha/dv) \cdot (dv/dt) ,$$

where

$$d\alpha/dv = -\frac{1}{C} \cdot \frac{d}{dv}\frac{di}{dv} = -\frac{1}{C}\frac{d^2i}{dv^2} ;$$

with all derivatives evaluated at $\alpha = o$. The value of $(d^2i/dv^2)_{\alpha=o}$ is a property of the dc characteristics of the tunnel diode. For a 1 mA Ge diode, it was measured as $-0.2\ A/V^2$.[50] Assuming that tunnel diodes have geometrically similar i vs v curves, in general this quantity will be proportional to the peak current, and

$$(d\alpha/dv)_{\alpha=o} = 200 \cdot I_p/C \qquad (V.4)$$

On the basis of this relation, and Fig. 18b with $\Lambda \equiv I_o/I_p$

$$V_1 = \left[\frac{-2I_o}{d^2i/dv^2} \right]^{\frac{1}{2}} = \Lambda^{\frac{1}{2}}/10 \qquad (V.5)$$

The quantity dv/dt is related to dy/dx, which in turn was numerically computed from Eq. (V.2). Values of $D \equiv (dy/dx)_{y=1}$ are shown in Fig. 21. The computed points can be fit reasonably well by the relationship

$$D = A^{2/3}(1 + A/8)^{-1/6} \qquad (V.6)$$

For small values of A, $D \rightarrow A^{2/3}$; and for large A, $D \rightarrow (2A)^{1/2}$.

From the definition of A, x, y, and Λ, and from equations (V.3), (V.4), and (V.6) we find

$$\tau_j = 0.2C^{2/3} I_p^{1/3} k^{-1/3} (1 + A/8)^{1/12} \qquad (V.7)$$

If

$$A/96 = 960^{-1} kC \left[1 + 1/(20R \cdot I_p)\right]^3 I_p^{-2} \Lambda^{-2/3} \ll 1, \qquad (V.8)$$

equation (V.7) can be approximated by

$$\tau_j \approx 0.2C^{2/3} I_p^{-1/3} k^{-1/3} , \qquad (V.9)$$

and the average jitter becomes

$$\sigma_j \equiv \tau_j/2 = 0.1C^{2/3} I_p^{-1/3} k^{-1/3} \qquad (V.10)$$

In order to have valid results, the normalized voltage across the tunnel diode has to reach 1 before time T. The required normalized time Ax_1 necessary to reach y = 1 is plotted in Fig. 22 as a function of A. The normalized time X corresponding to T is $X = I_o ST/(CV_1)$ and $AX = I_s/(I_o S^2)$.

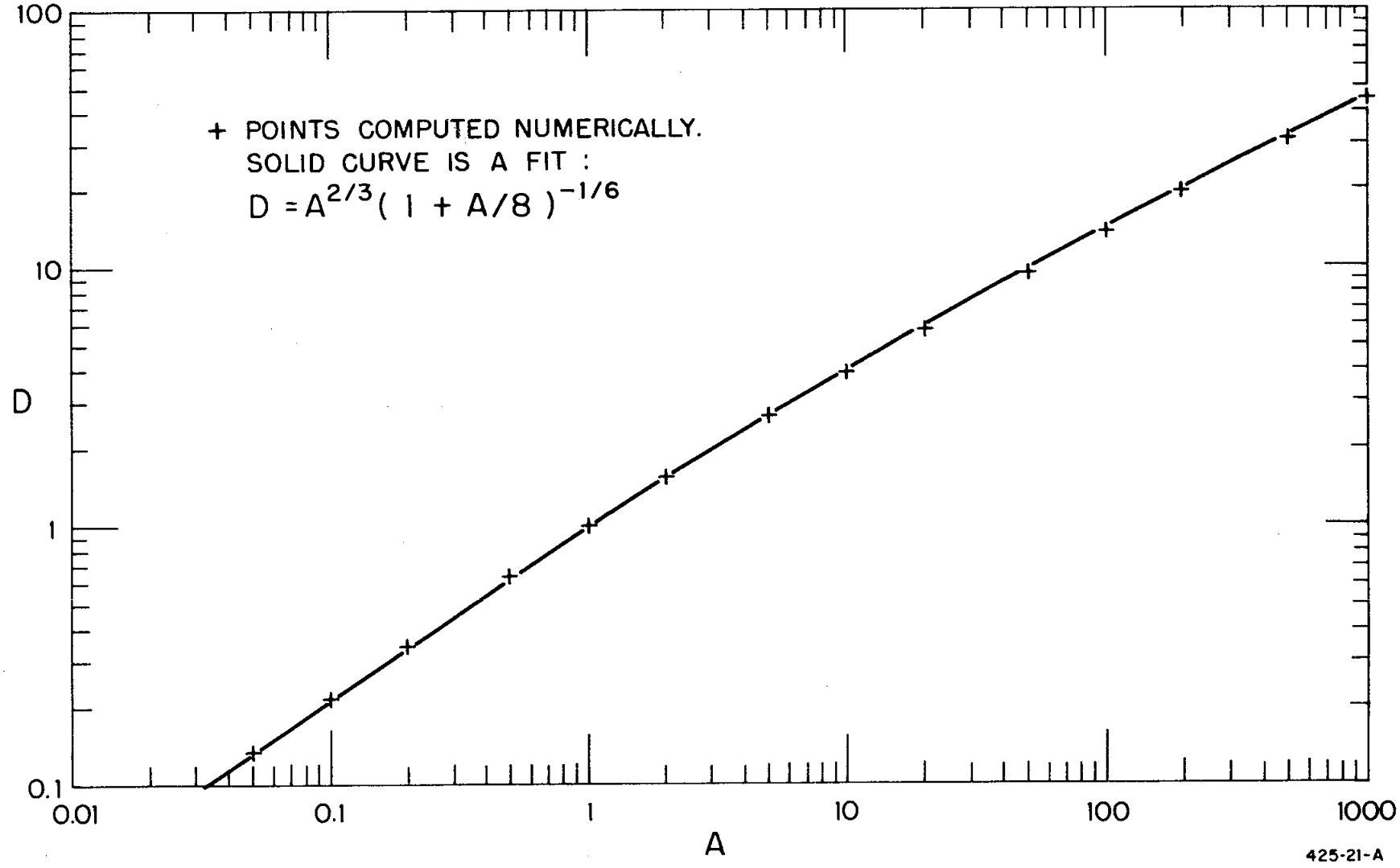

Fig. 21

DERIVATIVE $D \equiv (dy/dx)_{y=1}$ AS FUNCTION OF A, AS COMPUTED NUMERICALLY.

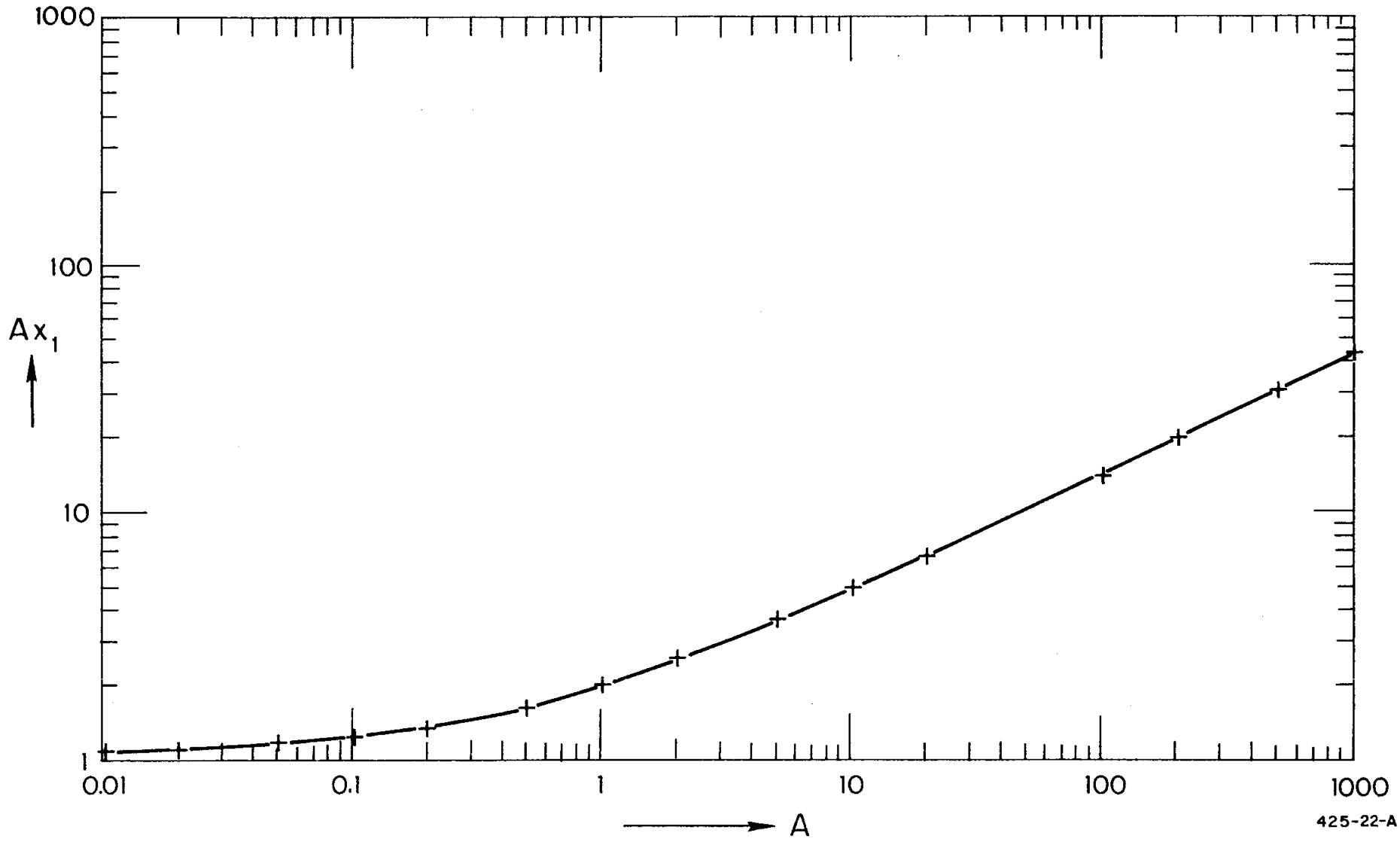

FIG. 22

NORMALIZED TIME Ax_1 REQUIRED TO REACH y = 1, AS FUNCTION OF A.

Thus

$$I_s/(I_o S^2) \geq Ax_1 \qquad (V.11)$$

is the condition for the validity of the above results.

C. Triggering Jitter of the Discriminator

When the two detector signals are separated by a finite time, the tunnel diode will or will not switch to its high state and a coincidence will or will not be registered depending on the time overlap of the clipped collector current signals. The earlier clipped signal will set the tunnel diode to the -40 mV, -3.4 mA point, the later clipped signal may switch it to its high state. The time jitter of the second transition will provide a contribution to the resolving time of the circuit.

For detector pulses with 1 nsec risetime, time T of Fig. 19c can be approximated by the 10% to 90% risetime t_r of Fig. 17, thus $k = I_s/T \approx I_s/t_r = 4.2\ \text{mA}/t_r$. The value of I_o is 5 mA - 3.4 mA = 1.6 mA and $\Lambda \equiv I_o/I_p = 1.6\ \text{mA}/5\ \text{mA} = 0.32$. The voltage $V_1 = \Lambda^{1/2}/10 \approx 50$ mV and the value of S can be computed as being S = 1.5. It can also be seen that the inequality (V.8) is valid in this case and hence Eq. (V.10) can be used:

$$\sigma_j = 0.1C^{2/3} \cdot I_p^{-1/3} \cdot k^{-1/3} = 0.1C^{2/3} \cdot t_r^{1/3} \cdot I_p^{-1/3} \cdot I_s^{-1/3} = 32(t_r)^{1/3}$$

where σ_j is in picoseconds and t_r is in nanoseconds. The values of A are given by $A \equiv kCV_1/(I_o^2 S^3) = I_s CV_1/(t_r I_o^2 S^3) = 25/t_r$; here t_r is in picoseconds. The condition of validity, inequality (V.11) becomes $Ax_1 \leq I_s/(I_o \cdot S^2) = 1.18$. Values of t_r, A, Ax_1, and σ_j are shown below for various values of V_{in}:

V_{in}(Volts)	t_r(nsec)	A	Ax_1	σ_j(psec)
1.0	0.7	0.035	1.12	33
1.5	0.45	0.055	1.15	28
2.0	0.35	0.07	1.18	25
3.0	0.2	0.125	1.25	< 25

The results of the computation are valid only if $Ax_1 \leq 1.18$, therefore for $V_{in} > 2$ volts the only information on the jitter is $\sigma_j < 25$ psec. Since the time jitter originating from the photomultiplier-tube pulse is in the 100-psec time range, the jitter of the tunnel diode could be neglected.

D. Feedthrough of Single Input Pulses

Pulse heights at the output of the 3-nsec pulse shaper following the discriminator circuit were measured for input pulses with -1.6 V height and 1-nsec risetime. (See Section IV.C.) The ratio of the pulse heights measured for coincident and single input pulses was 5 for clipping lengths of longer than L = 15 cm ($\doteqdot$ 0.5 nsec) and 4 for a clipping length of L = 9 cm ($\doteqdot$ 0.3 nsec).

VI. CONSTRUCTION

The two input limiters were constructed in a modified locking-type coaxial T-adapter.* A photograph of the construction technique is shown in Fig. 23. Connections to the inputs, to the output, and to the clipping line are made through four 50-Ω coaxial connectors. A multiconductor shielded power cable connects to the power supply via decoupling filters. Special care was taken to keep signal wires as short as possible.

* General Radio Type 874-TL.

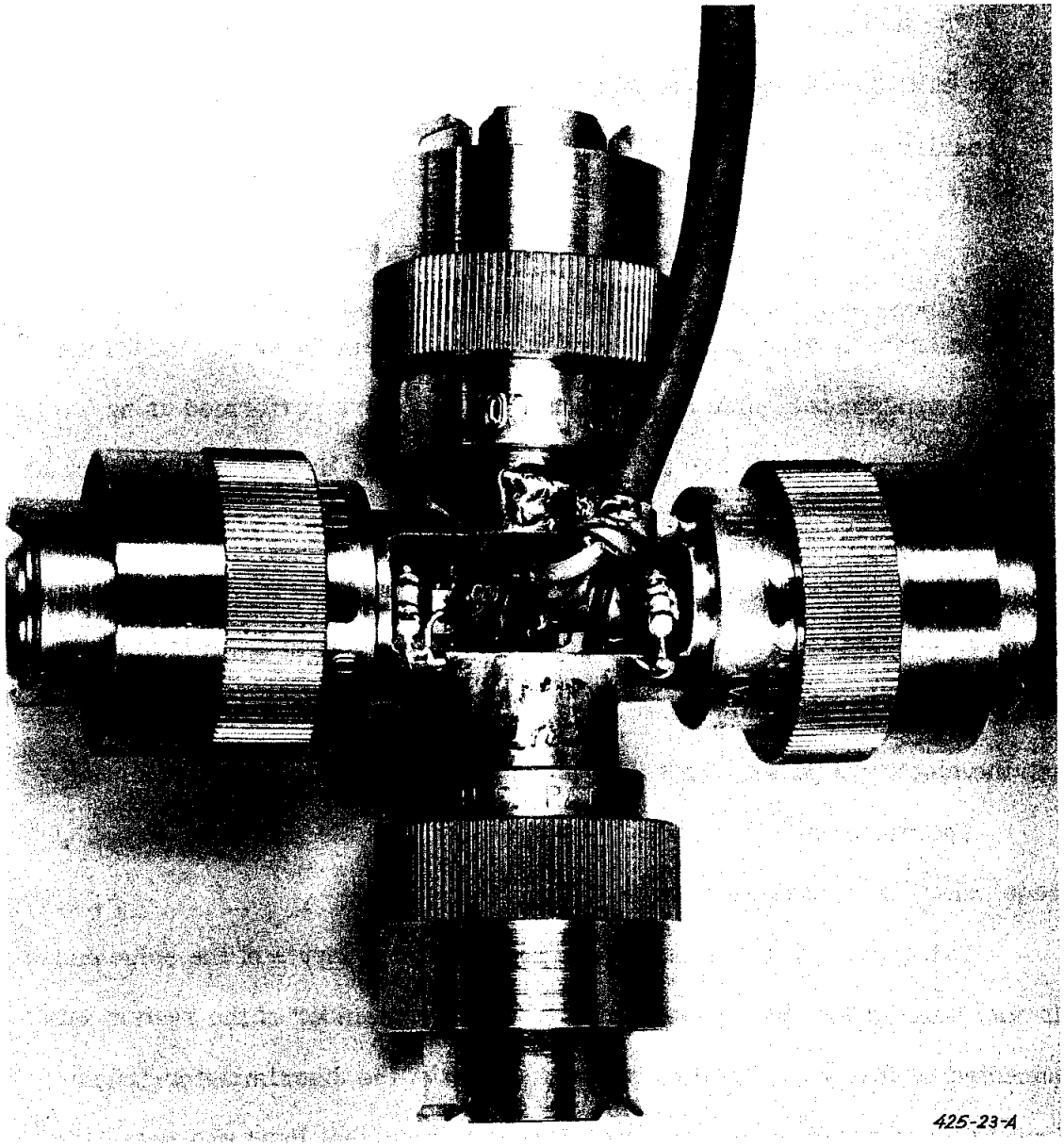

Fig. 23

A PHOTOGRAPH OF THE LIMITER. Magnification is approximately 1:2.

The tunnel diode discriminator, the 3-nsec shaper, and the × 10 amplifier are built in individual insertion units.* All interconnections are made by 50-Ω coaxial cables terminated by the circuitry at the receiving end.

VII. PERFORMANCE MEASUREMENTS

In order to estimate the behavior of the system under the conditions of an actual experiment, coincidence measurements were performed using the light pulser shown in Figs. 24 and 25.** The source of the light is a 5-kV spark between two closing contacts in high pressure mercury atmosphere; the contacts are operated at a rate of 60 Hz by an externally mounted coil. The waveform of the spark current is shown in Fig. 26. Due in part to light emitted by the excited states of the mercury atom[51] the length of the actual light pulse is longer than the electrical pulse. This difference will be neglected in the following.

The photomultiplier tubes were operated with the circuit of Fig. 27. The anode pulses are shown in Fig. 28.

The anodes of the tubes were connected to the inputs of the coincidence circuit, one through an adjustable delay.† The remainder of the system was connected as in Fig. 7. The output pulse width of the discriminator/trigger circuit was adjusted to 60 nsec as required by the signal input characteristics of the particular counter used.†† The time reference output of the light pulser was attenuated and entered into the external time base input of the counter via

---

* General Radio Type 874-X.

** A model 961F pulse generator, manufactured by Huggins Laboratories, Inc., Sunnyvale, California, was used as a light source. The mercury capsule assembly was modified to obtain a shorter pulse.

† General Radio Type 874-LTL.

†† Hewlett-Packard Type HP5245L.

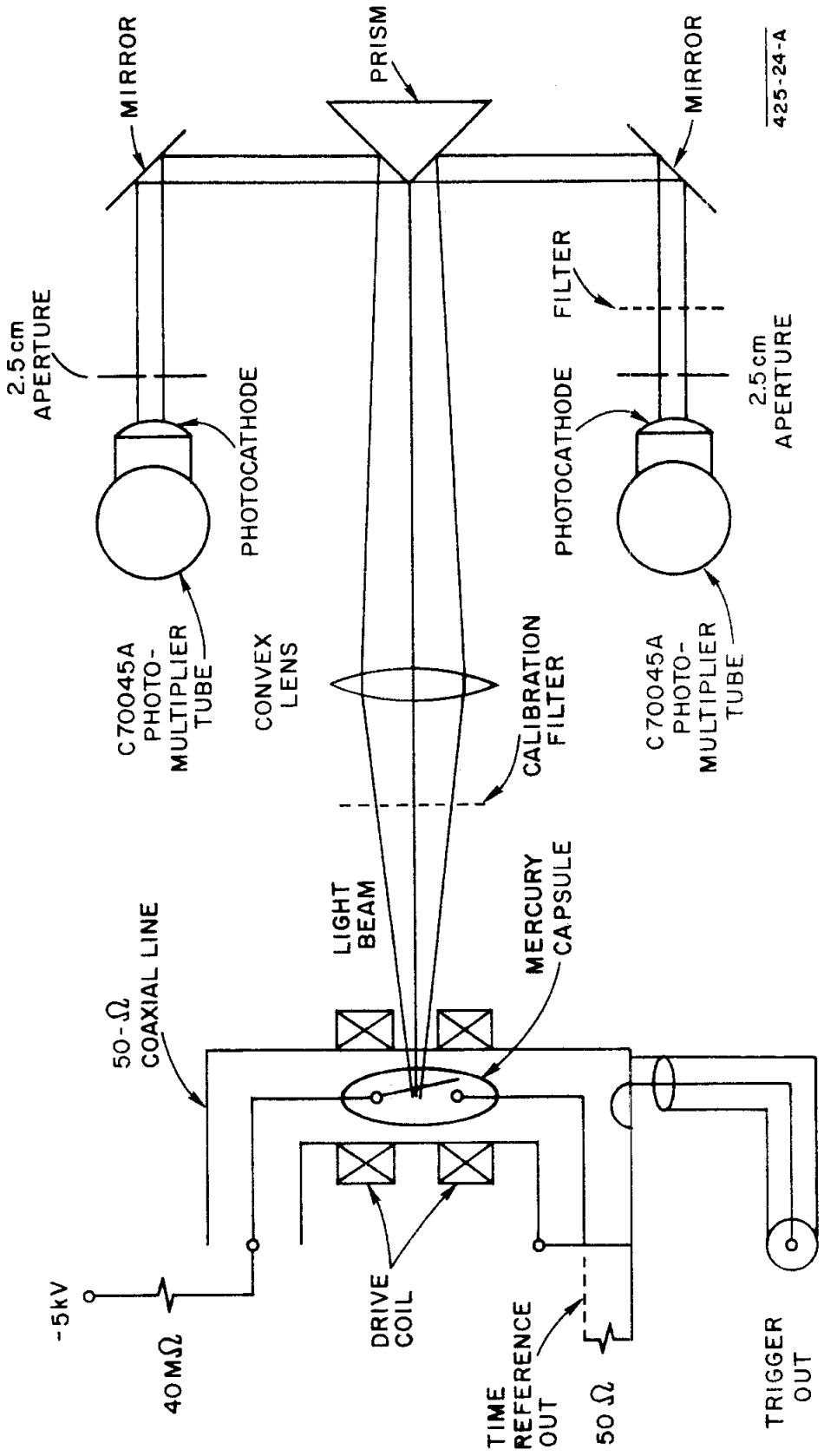

FIG. 24

LAYOUT OF THE LIGHT PULSER.

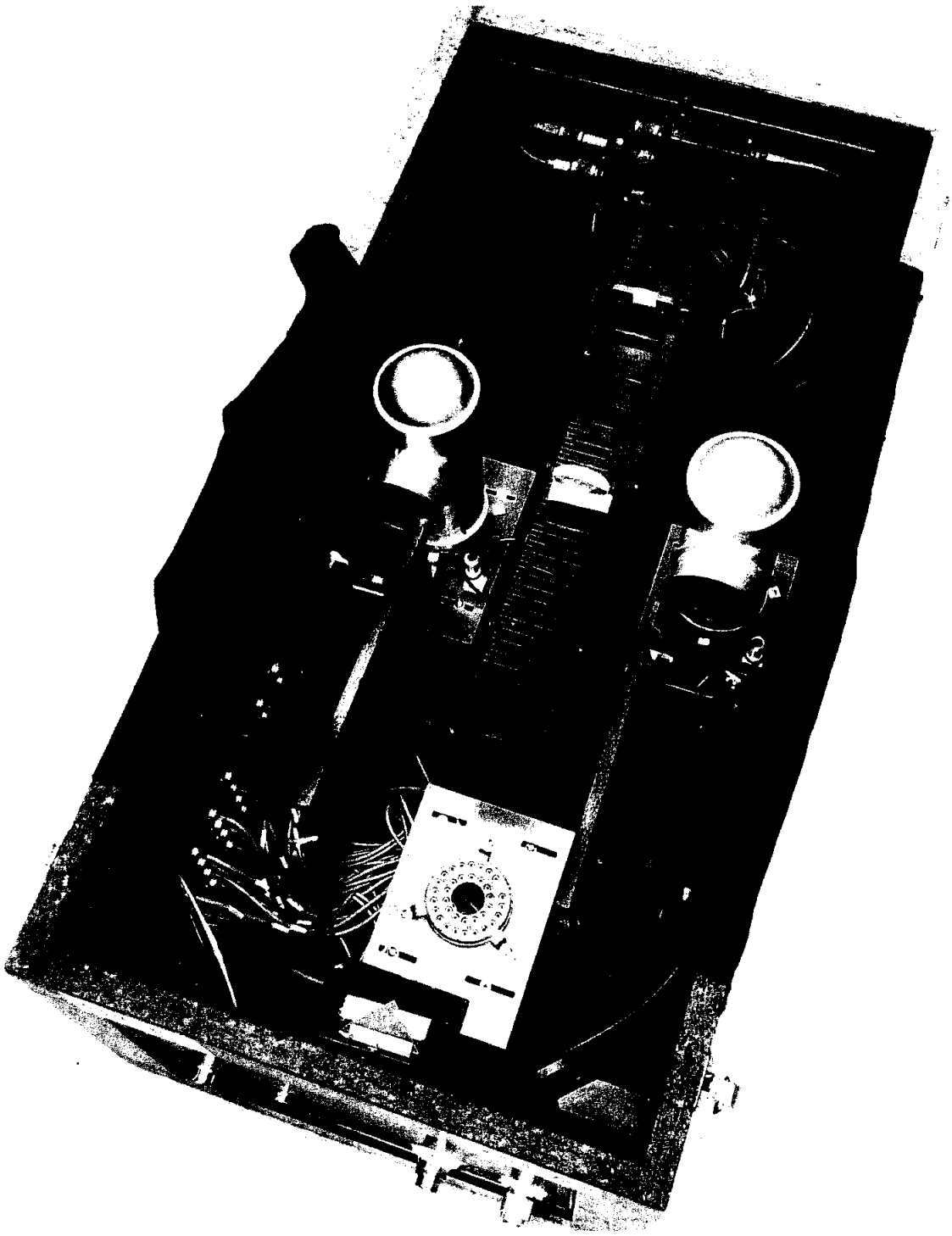

Fig. 25

A PHOTOGRAPH OF THE LIGHT PULSER. The unit is 90 cm long, 40 cm wide and 30 cm high. The light source is at the upper end of the photograph, followed by a calibration filter, lens, a prism at lower end of the photograph, mirrors, diaphragms and photomultiplier tubes. Empty socket was not utilized in the measurement described here. Black cloth light baffles are folded over sides.

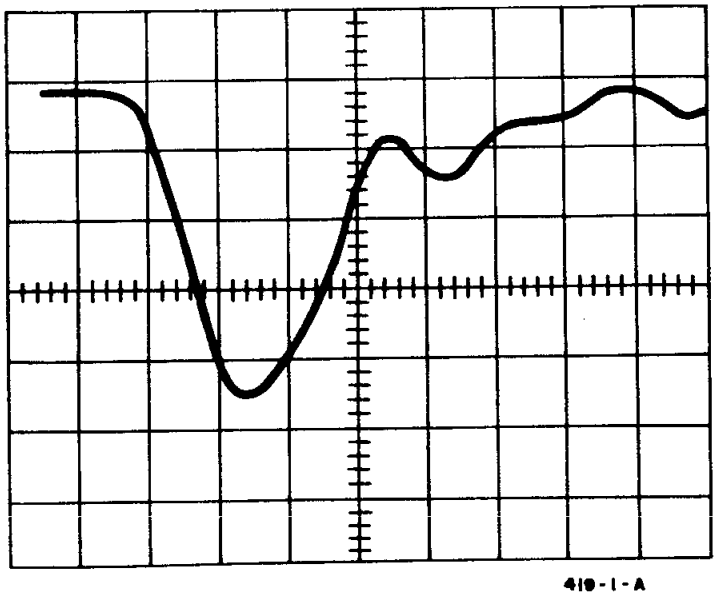

FIG. 26

TIME REFERENCE OUTPUT PULSE WAVEFORM. Sweep speed: 0.4 nsec/cm, Sensitivity (through attenuators): 500 V/cm.

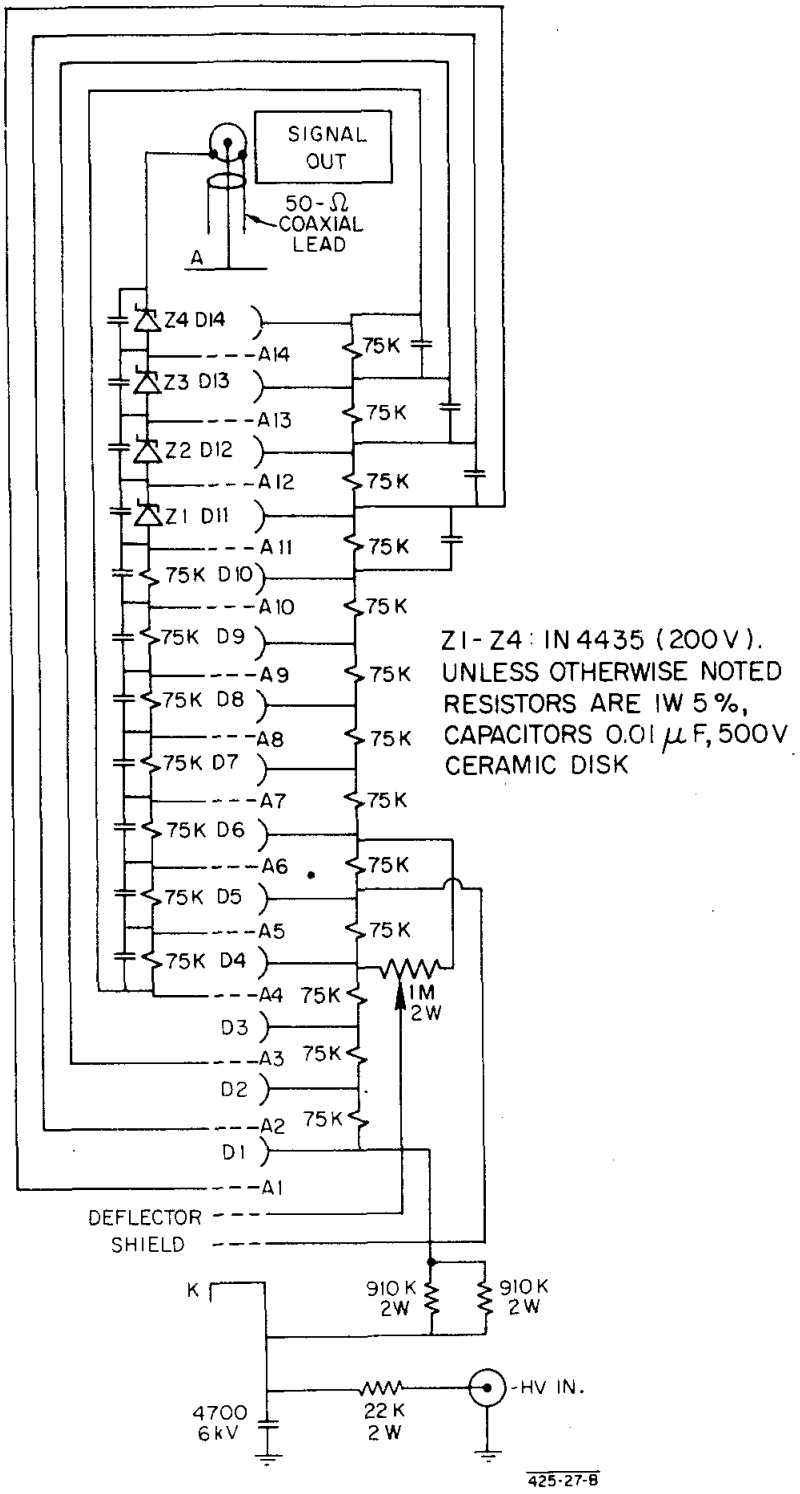

FIG. 27

PHOTOMULTIPLIER TUBE BASE FOR C70045A. SCHEMATIC DIAGRAM.

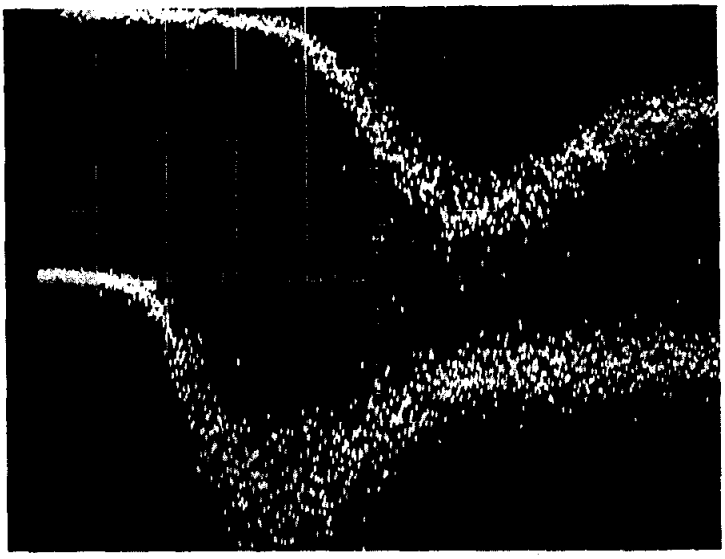

FIG. 28

WAVEFORMS OF THE ANODE PULSES OF THE PHOTOMULTIPLIER-TUBES. High voltages on the tubes were 5.6 kV and 6 kV. Type 561 oscilloscope, type 4S2 preamp (0.1 nsec risetime); Sensitivity : 0.5 V / cm, Sweep speed : 0.5 nsec/cm.

an auxiliary discriminator/trigger circuit with a 16 μsec pulse width. The counter was preset to count signal input pulses for a period of 1000 time-base input pulses.

Coincidence counts for 1000 pulses* were measured as functions of the relative delay of the two photomultiplier tube signals for different bias settings of the discriminator/trigger circuit of Fig. 7. The results of the measurements are shown in Fig. 29. It can be seen that when 10,000 photons/event are available, a resolving time of $\tau = 0.3$ nsec is attainable.

VIII. ANALYSIS OF THE PERFORMANCE

The time jitter contributed by the time spread of the light pulse impinging on the photocathode and by the photomultiplier tube has been recently calculated[54] for light pulses of the form

$$I(t) = \exp(-\mu t) - \exp(-\gamma\mu t) \qquad \text{(VIII. 1)}$$

The time jitter can be expressed as

$$\sigma_r = \sqrt{2} \cdot \mu^{-1} \cdot N^{-\frac{1}{2}} \cdot r \cdot f \qquad \text{(VIII. 2)}$$

Here N is the number of photoelectrons emitted from the photocathode available for timing; r takes into account the statistics of the secondary-emission multiplication process of the dynodes. (See Appendix). The factor f is a function of γ, $\sigma\mu$, σ'/σ, and of the fraction of the photomultiplier-tube pulse utilized for the coincidence, and it depends on the method of timing.

---

* Each pulse supplied approximately 10,000 photons onto each photocathode. This calibration was performed by single photoelectron measurement techniques similar to that described in Ref. 52 and 53.

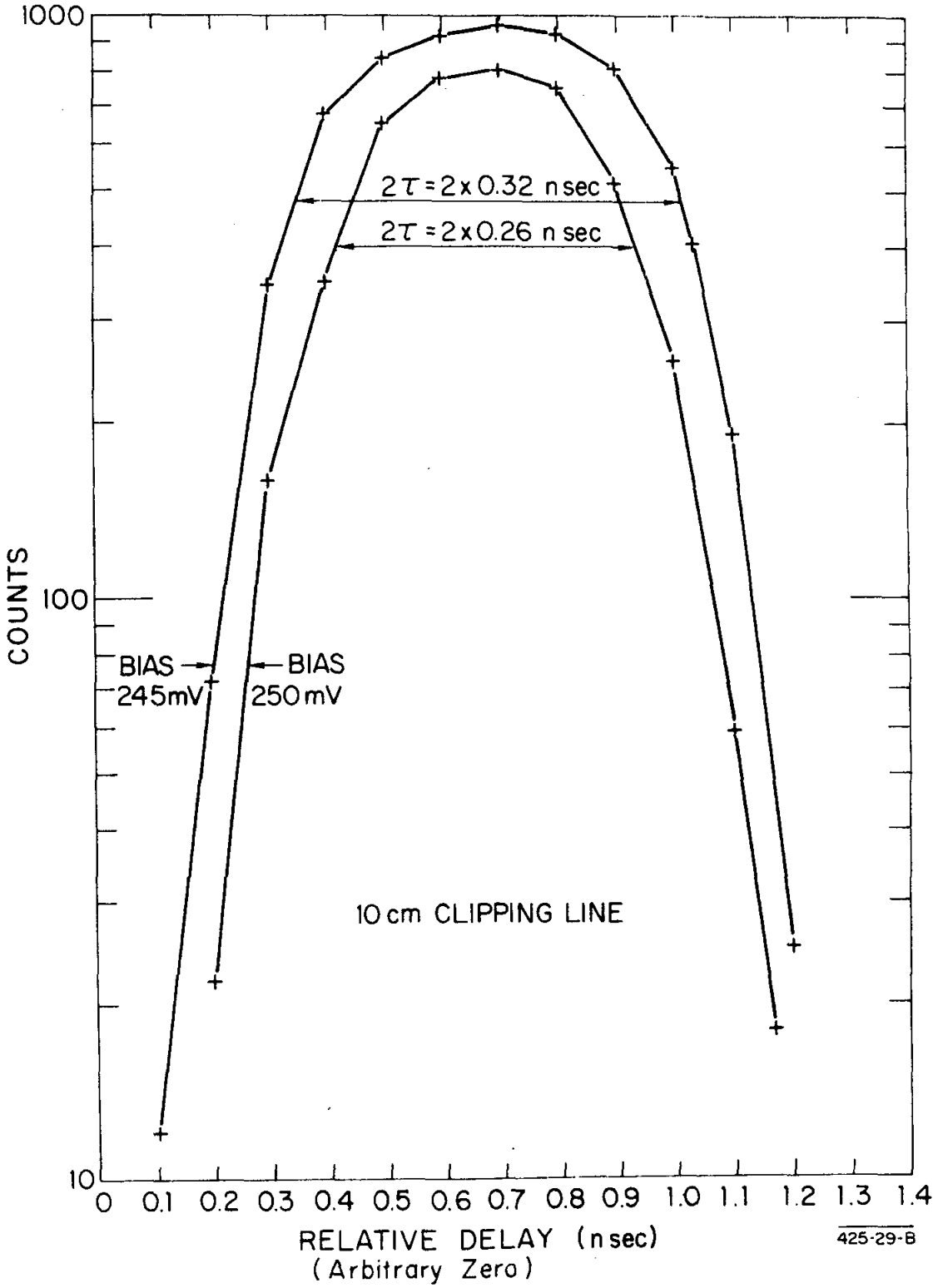

Fig. 29

COINCIDENCE COUNTS FOR 1000 LIGHT PULSES, AS FUNCTION OF THE RELATIVE DELAY BETWEEN THE TWO INPUTS (ARBITRARY ZERO), WITH THE DISCRIMINATOR / TRIGGER BIAS SETTING AS PARAMETER. The curves fall off with a slope of 100 psec/decade.

The waveform of Fig. 26 can be approximated by Eq. (VIII.1) with $1/\mu \approx 750$ psec and $\gamma = 2.5$. From data from Sec. III above it follows

$$\sigma\mu = 135 \text{ psec}/750 \text{ psec} \approx 1/6$$

and

$$\sigma'/\sigma = 30 \text{ psec}/135 \text{ psec} \approx 1/4$$

In the measurements performed the number of photoelectrons emitted by the photocathode was in the vicinity of 2000 per pulse. However, only a fraction of these are available for timing. The fraction of the pulse utilized for the coincidence is not precisely defined for the mode of operation employed in this circuit. It will be assumed (Cf. Figs. 17 and 28) that the timing is determined at the 50% pulse height and that about 5% of the emitted photoelectrons, i.e., N = 100, are utilized for timing purposes. With these data, for integral mode of operation we get by extrapolation of Fig. 8c of Ref. 54 an f in the vicinity of 2.

With r = 1.12 (obtained from the Appendix) Eq. (VIII.2) becomes

$$\sigma_r = \sqrt{2} \cdot 750 \text{ psec} \cdot 100^{-\frac{1}{2}} \cdot 1.12 \cdot 2 \approx 235 \text{ psec} \qquad \text{(VIII.3)}$$

Additional contribution comes from the tunnel diode triggering jitter (see Sec. V.C. above), thus the resolving time τ can be computed as

$$\tau = 1.17\left[\sigma_r^2 + \sigma_j^2\right]^{\frac{1}{2}} = 1.17\left[235^2 + 28^2\right]^{\frac{1}{2}} \text{ psec} \approx 237 \text{ psec}$$

in reasonable agreement with the measured value of 300 psec. This resolving time might be improved by the use of shorter light pulses and by a better utilization of the available pulse from the photomultiplier tube.

APPENDIX

The standard deviation of the time spread of a system consisting of a photocathode and n subsequent dynodes, assuming Gaussian processes, can be written as

$$\sigma_m = N^{-\frac{1}{2}} \left[1 + \frac{1}{m_1} + \frac{1}{m_1 m_2} + \frac{1}{m_1 m_2 m_3} + \ldots + \frac{1}{m_1 m_2 m_3 \ldots m_n} \right]^{\frac{1}{2}} \equiv N^{-\frac{1}{2}} r \tag{A.1}$$

Here N is the number of photoelectrons per pulse emitted by the photocathode, m_1 through m_n are the secondary electron multiplication factors of dynodes 1 through n, respectively.

In the case when all secondary emission multiplication factors are equal:

$$m_1 = m_2 = m_3 = \ldots = m_n \equiv m$$

$$r = \left[1 + \frac{1}{m} + \frac{1}{m^2} + \frac{1}{m^3} + \ldots + \frac{1}{m^n} \right]^{\frac{1}{2}} = \left[1 + \frac{m^n - 1}{m^n (m-1)} \right]^{\frac{1}{2}} \tag{A.2}$$

In the case when all secondary emission multiplication factors except m_1 are equal:

$$m_1 \neq m_2 = m_3 = \ldots = m_n \equiv m,$$

$$r = \left[1 + \frac{1}{m_1} + \frac{1}{m_1 m} + \frac{1}{m_1 m^2} + \ldots \frac{1}{m_1 m^{n-1}} \right]^{\frac{1}{2}} = \left(1 + \frac{1}{m_1} \left[1 + \frac{m^{n-1} - 1}{m^{n-1}(m-1)} \right] \right)^{\frac{1}{2}} \tag{A.3}$$

For the C70045A operated with the circuit of Fig. 27, $m_1 \approx 6$ and $m_2 = m_3 = \ldots = m_n = m \approx 3$, thus from Eq. (A.3)

$$r = \left(1 + \frac{1}{6} \left[1 + \frac{3^{13}-1}{3^{13}(3-1)} \right] \right)^{\frac{1}{2}} \approx 1.12$$

REFERENCES

1. W. Bothe, Zur Vereinfachung von Koinzidenzzahlungen, Zeitschrift fur Physik 59 (1929) 1-5.
2. R. E. Bell, Nuclear Particle Detection: Fast Electronics, Annual Review of Nuclear Science, Vol. 4, Annual Review, Stanford, 1954, 93-110.
3. E. Baldinger and W. Franzen, Amplitude and Time Measurement in Nuclear Physics, Advances in Electronics and Electron Physics, Vol. VIII, Academic Press, New York (1956) 255-315.
4. S. DeBenedetti and R. W. Findley, The Coincidence Method, Nuclear Instrumentation II, Encyclopedia of Physics, Vol, 45, Springer, 1958.
5. I. A. D. Lewis and F. H. Wells, Millimicrosecond Pulse Techniques, Pergamon Press, 1959.
6. R. L. Chase, Nuclear Pulse Spectrometry, McGraw-Hill, 1961.
7. R. E. Bell, Coincidence Techniques and the Measurement of Short Mean Lives, Alpha-, Beta-, and Gamma-Ray Spectroscopy, K. Siegbahn, Editor, North Holland Publishing Co., Amsterdam, 1965.
8. R. L. Anderson and B. D. McDaniel, A Sub-Nanosecond Time-of-Flight Circuit Utilizing the Inherent Modulation of a Synchrotron Beam, Nucl. Instr. and Methods 21 (1963) 235-242.
9. R. L. Garwin, A Useful Fast Coincidence Circuit, Rev. Sci. Instr. 21 (1950) 569.
10. R. E. Bell, R. L. Graham and H. E. Petch, Design and Use of a Coincidence Circuit of Short Resolving Time, Can. J. Phys. 30 (1952) 35-52.
11. W. A. Wenzel, Millimicrosecond Coincidence Circuit for High Speed Counting, UCRL-8000, University of California, Berkeley (October 1957).

12. V. L. Fitch, Semiconductor Devices in Coincidence Circuits, Symposium on Advances in Fast-Pulse Techniques for Nuclear Counting, Report UCRL-8706, University of California (February 1959) 118-119.

13. V. L. Fitch, Applications of Transistors in Counter Experiments, International Conference on High Energy Accelerators and Instrumentation, CERN, European Organization for Nuclear Research, Geneva (1959) 601-604.

14. R. H. Miller, Simplified Coincidence Circuits Using Transistors and Diodes, Symposium on Advances in Fast-Pulse Techniques for Nuclear Counting, Report UCRL-8706, University of California (February 1959) 120-125 and Rev. Sci. Instr. 30 (1959) 395-398.

15. R. H. Miller, Transistorized Coincidence Circuit for π-e Experiment, Rev. Sci. Instr. 31 (1960) 1047-1051.

16. R. M. Sugarman, Nonsaturating Transistor Circuitry for Nanosecond Pulses, IRE Transactions on Nuclear Science, Vol. NS-7, No. 1 (1960) 23-28.

17. A. Barna, J. H. Marshall, and M. Sands, A Nanosecond Coincidence Circuit Using Transistors, International Conference on High Energy Accelerators and Instrumentation, CERN, European Organization for Nuclear Research, Geneva (1959) 604-614 and Nucl. Instr. and Methods 7 (1960) 124-134.

18. A. Barna, J. H. Marshall and D. F. Torzewski, Printed-Circuit Modular Instrumentation System, Rev. Sci. Instr. 36 (1965) 166-173.

19. A. Barna and D. F. Torzewski, Modular Instrumentation Handbook, Part I, Report EFINS 63-83 (1963) and Part II, Report EFINS 64-66 (1964), University of Chicago.

20. S. C. Baker, H. G. Jackson and D. A. Mack, Transistor Counting Systems for Scintillation Detectors, IRE Trans. Nucl. Sci. NS-7, No. 2-3 (1960) 89-95.

21. R. M. Sugarman and W. A. Higinbotham, Nanosecond Counter Circuits, Proceedings of an International Conference on Instrumentation for High-Energy Physics, University of California (September 1960), Interscience Publishers, New York, London (1961) 54-58.

22. R. Sugarman, W. A. Higinbotham, and A. H. Yonda, 100-Mc Counting System, Nuclear Electronics, Proceedings of the Belgrade Conference (1961) Vol. III,3-13.

23. R. M. Sugarman, A. C. Melissinos, and J. S. Weaver, Performance of a Transistorized Nanosecond Counting System, Proceedings of an International Conference on Instrumentation for High-Energy Physics, University of California (September 1960), Interscience Publishers, New York, London (1961) 59-61.

24. R. Sugarman, F. C. Merritt, and W. A. Higinbotham, Nanosecond Counter Circuit Manual, Report BNL 711 (T-248), Brookhaven National Laboratory, February 1962.

25. Q. A. Kerns, A. E. Bjerke, and T. A. Nunamaker, Tunnel Diode Discriminator, Proceedings of an International Conference on Instrumentation for High-Energy Physics, University of California (September 1960), Interscience Publishers, New York, London (1961) 62-63.

26. C. Wiegand, Electronic Counter Techniques at Berkeley, Nucl. Inst. and Methods 20 (1963) 313-318.

27. S. Gorodetzky, A. Muser, J. Zen, and R. Armbruster, Sur un Circuit Rapide de Mise en Forme a Seuil Reglable Utilisant des Diodes Tunnel, Nucl. Instr. and Methods 13 (1961) 282-286.

28. S. Gorodetzky, A. Muser, J. Zen, and R. Armbruster, Circuit de Coincidence a Diodes Tunnel, Nucl. Instr. and Methods 14 (1961) 205-208.

29. A. Whetstone and S. Kounosu, Nanosecond Coincidence Circuit Using Tunnel Diodes, Rev. Sci. Instr. 33 (1962) 423-428.

30. A. L. Whetstone, Survey of Nanosecond Techniques, IRE Transactions on Nuclear Science NS-9 No. 3 (June 1962) 280-284.

31. A. L. Whetstone, Improving the Tunnel Diode Univibrator, Rev. Sci. Instr. 34 (1963) 412-413.

32. Master Electronics Handbook, University of Illinois, Elementary Particle Physics Research (1963).

33. M 100 Modular Counting System, Edgerton, Germeshausen and Grier, Inc., Salem, Mass. (1963).

34. Nanologic System 100, Chronetics, Inc., Yonkers, N.Y. (1963).

35. A. F. Dunaitsev, A Nanosecond Multiple Coincidence-Anticoincidence Circuit Using Tunnel Diodes and Transistors, Pribory i Tekhnika Eksperimenta, 1964, No. 6, 77-82.

36. M. Birk, Q. A. Kerns and R. F. Tusting, Evaluation of the C70045A High-Speed Photomultiplier, IEEE Transactions on Nuclear Science, Vol. NS-11, No. 3 (June 1964) 129-138.

37. G. A. Morton and R. M. Matheson, A Fast Photomultiplier and Coincidence System for Precise Time Measurements, Nuclear Electronics, International Atomic Energy Agency, Vienna (1959) 201-208.

38. Proposed Technical Objective for RCA Photomultiplier Type C70045A, Radio Corporation of America, TL 134, 11/60.

39. Electron Tube Division, Radio Corporation of America, Development of a Photomultiplier Having a Pulse Risetime Less Than 5×10^{-10} second, Final Report, Contract AT(30-1)-3032, June 1963.

40. R. M. Matheson, Recent Photomultiplier Developments at RCA, IEEE Transactions on Nuclear Science, Vol. NS-11, No. 3 (June 1964) 64-71.

41. MD1132, MD1132F, NPN Dual Transistors, Multiple Devices, Motorola Semiconductors, DS4512 (August 1964).

42. Data Sheet and Procurement Specifications, 2N918 Fairchild NPN Double Diffused Silicon Planar Epitaxial Transistor, Fairchild Semiconductor, 1963.

43. J. G. Linvill, Models of Transistors and Diodes, McGraw-Hill, 1963.

44. W. C. Elmore and M. L. Sands, Electronics, Experimental Techniques, McGraw-Hill, 1949.

45. General Electric, Semiconductor References, 70.26 (2/64).

46. G. Infante and F. Pandarese, The Tunnel Diode as a Threshold Device: Theory and Application, Nuclear Electronics, Proceedings of the Belgrade Conference, 1961, Vol. III, 29-40.

47. F. Lacour, Utilisation des Diodes Tunnel en Electronique Impulsionelle, Nuclear Electronics, Proceedings of the Belgrade Conference, 1961, Vol. III, 179-193.

48. W. A. Edson, Noise in Oscillators, Proceedings of the IRE, Vol. 48 (August 1960) 1454-1466.

49. Chu-Sun Yen, On the Trigger-Time Jitter of a Regenerative Pulse Circuit, IEEE Convention Records Vol. II, Part 2, 1963.

50. E. Baldinger and U. Spycher, Ein Einfaches Testgerat zur Bestimmung der Parameter von Tunneldioden, Helv. Phys. Acta 35 (1962) 232-237.

51. C. H. Corliss and W. R. Bozman, Experimental Transition Probabilities for Spectral Lines of Seventy Elements, National Bureau of Standards Monograph 53, 1962.

52. Q. A. Kerns, F. A. Kirsten, and G. C. Cox, Generator of Nanosecond Light Pulses for Phototube Testing, Rev. Sci. Instr. 30 (1959) 31-36.

53. F. A. Kirsten, Multiplier Phototube Testing, Fast Pulse Techniques in Nuclear Counting, UCRL-8706, University of California, Berkeley (February 1959) 1-7.

54. L. G. Hyman, Time Resolution of Photomultiplier Systems, Rev. Sci. Instr. 36 (1965) 193-196.